Cosmological Radiative Transfer Comparison Project

Ilian Iliev
ITP, University of Zurich

Project website: http://www.cita.utoronto.ca/~iliev/rtwiki/doku.php

Motivation and Basic Strategy

- The full RT problem is very expensive, multy-dimensional problem, so approximations are inevitably required.
- Our aim is to validate our codes and evaluate their reliability and limitations, on the way creating a development testbed for future codes.
- Very few, simplified problems have exact analytical solutions to check RT codes against.
- Next best approach – compare results from independent codes on common problems.
- Problems: simple and clean, of increasing difficulty, involving astrophysically-interesting situations.
- Everybody is welcomed to join. Regular workshops. Results published in series of papers and at a

Organization

- Open project: everybody free to join.
- Open-ended project – continually updated and new tests/new physics added.
- Any problem would be considered, but for inclusion min 3 codes should do it.
- Regular workshops (2 to date, another soon).
- Papers on results published after each stage of the project is completed.
- Project and analysis coordinated by a single person, with help from

Mon. Not. R. Astron. Soc. **000**, 1 (2006) Printed 26 June 2006 (MN LaTeX style file v2.2)

Cosmological Radiative Transfer Codes Comparison Project I: The Static Density Field Tests

Ilian T. Iliev[1⋆], Benedetta Ciardi[2], Marcelo A. Alvarez[3], Antonella Maselli[2], Andrea Ferrara[4], Nickolay Y. Gnedin[5,6], Garrelt Mellema[7,8], Taishi Nakamoto[9], Michael L. Norman[10], Alexei O. Razoumov[11], Erik-Jan Rijkhorst[8], Jelle Ritzerveld[8], Paul R. Shapiro[3], Hajime Susa[12], Masayuki Umemura[9], Daniel J. Whalen[10,13]

[1] *Canadian Institute for Theoretical Astrophysics, University of Toronto, 60 St. George Street, Toronto, ON M5S 3H8, Canada*
[2] *Max-Planck-Institut für Astrophysik, 85741 Garching, Germany*
[3] *Department of Astronomy, University of Texas, Austin, TX 78712-1083, U.S.A.*
[4] *SISSA/International School for Advanced Studies, Via Beirut 4, 34014 Trieste, Italy*
[5] *Fermilab, MS209, P.O. 500, Batavia, IL 60510, U.S.A.*
[6] *Department of Astronomy & Astrophysics, The University of Chicago, Chicago, IL 60637, U.S.A.*
[7] *ASTRON, P.O. Box 1, NL-7990 AA Dwingeloo, The Netherlands*
[8] *Sterrewacht Leiden, P.O. Box 9513, NL-2300 RA Leiden, The Netherlands*
[9] *Center for Computational Sciences, University of Tsukuba, Tsukuba, Ibaraki 305-8577, Japan*
[10] *Center for Astrophysics and Space Sciences, University of California, San Diego, 9500 Gilman Drive, La Jolla, CA 92093-0424, U.S.A.*
[11] *Physics Division, Oak Ridge National Laboratory, Oak Ridge, TN 37831-6354, U.S.A.*
[12] *Department of Physics, College of Science, Rikkyo University, 3-34-1 Nishi-Ikebukuro, Toshimaku, Tokyo, Japan*
[13] *T-6 Theoretical Astrophysics, Los Alamos National Laboratory, Los Alamos, NM 87545, U.S.A.*

11 codes (new ones constantly joining), including ray-tracing (long and short char.), Monte-Carlo, moment; fixed, AMR, unstructured grids, and no grid (particle-based): cover most of the spectrum of possible approaches.

Mon. Not. R. Astron. Soc. **000**, 1 (2006) Printed 8 May 2007 (MN LaTeX style file v2.2)

WORK IN PROGRESS

Cosmological Radiative Transfer Codes Comparison Project II: The Radiative-Hydrodynamic Tests

Ilian T. Iliev[1★], Kyungjin Ahn[2], Sunghye Baek[3], Nickolay Y. Gnedin[4], Andrey V. Kravtsov[5], Garrelt Mellema[6], Michael Norman[7], Milan Raicevic[8], Daisuke Sato[9] Paul R. Shapiro[2], Benoit Semelin[3], Joseph Smidt[10], Hajime Susa[9], Tom Theuns[8], Masayuki Umemura[11], Daniel Whalen[12]

[1] *Canadian Institute for Theoretical Astrophysics, University of Toronto, 60 St. George Street, Toronto, ON M5S 3H8, Canada*
[2] *Department of Astronomy, University of Texas, Austin, TX 78712-1083, U.S.A.*
[3] *LERMA, Observatoire de Paris, 77 av Denfert Rochereau, 75014 Paris*
[4] *Fermilab, MS209, P.O. 500, Batavia, IL 60510, U.S.A.*
[5] *Dept. of Astronomy and Astrophysics, Center for Cosmological Physics, The University of Chicago, Chicago, IL 60637, U.S.A.*
[6] *Stockholm Observatory, AlbaNova University Center, Stockholm University, SE-106 91 Stockholm, Sweden*
[7] *Center for Astrophysics and Space Sciences, University of California, San Diego, 9500 Gilman Drive, La Jolla, CA 92093-0424, U.S.A.*
[8] *Institute for Computational Cosmology, Durham, U.K.*
[9] *Department of Physics, College of Science, Rikkyo University, 3-34-1 Nishi-Ikebukuro, Toshimaku, Tokyo, Japan*
[10] *Brigham Young University, Department of Physics and Astronomy N283 ESC, Provo, UT 84602, U.S.A.*
[11] *Center for Computational Sciences, University of Tsukuba, Tsukuba, Ibaraki 305-8577, Japan*
[12] *T-6 Theoretical Astrophysics, Los Alamos National Laboratory, Los Alamos, NM 87545, U.S.A.*

8 codes (to date): varieties of ray-tracing, Monte-Carlo (?), moments, particles; hydro: Eulerian, Lagrangean, SPH, AMR, Riemann solver; many are parallelized

Radiative Transfer Comparison Project Wiki

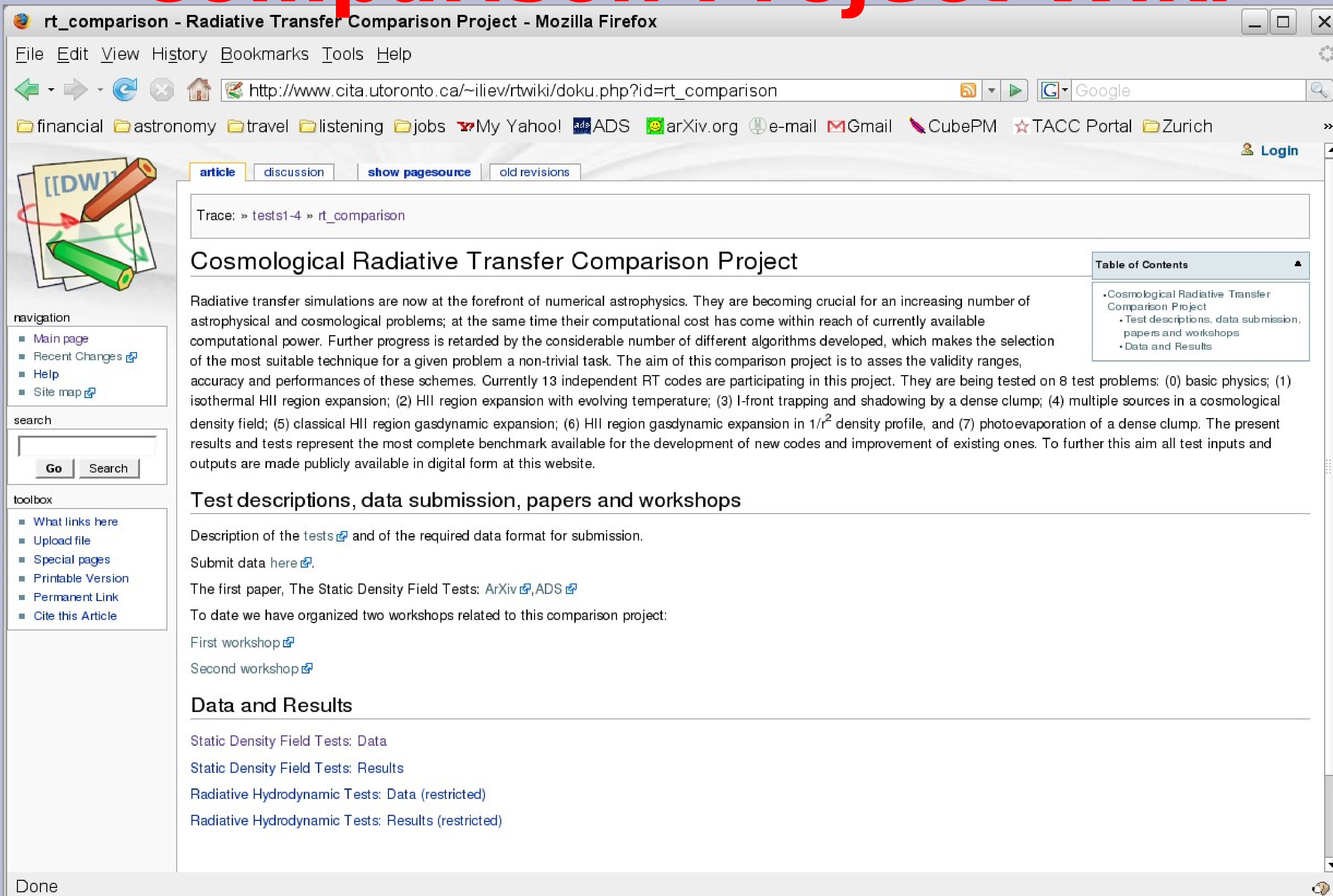
rt_comparison - Radiative Transfer Comparison Project - Mozilla Firefox

File Edit View History Bookmarks Tools Help

http://www.cita.utoronto.ca/~iliev/rtwiki/doku.php?id=rt_comparison

financial astronomy travel listening jobs My Yahoo! ADS arXiv.org e-mail Gmail CubePM TACC Portal Zurich

Login

article | discussion | show pagesource | old revisions

navigation
- Main page
- Recent Changes
- Help
- Site map

search

Go Search

toolbox
- What links here
- Upload file
- Special pages
- Printable Version
- Permanent Link
- Cite this Article

Trace: » tests1-4 » rt_comparison

Cosmological Radiative Transfer Comparison Project

Table of Contents

Radiative transfer simulations are now at the forefront of numerical astrophysics. They are becoming crucial for an increasing number of astrophysical and cosmological problems; at the same time their computational cost has come within reach of currently available computational power. Further progress is retarded by the considerable number of different algorithms developed, which makes the selection of the most suitable technique for a given problem a non-trivial task. The aim of this comparison project is to asses the validity ranges, accuracy and performances of these schemes. Currently 13 independent RT codes are participating in this project. They are being tested on 8 test problems: (0) basic physics; (1) isothermal HII region expansion; (2) HII region expansion with evolving temperature; (3) I-front trapping and shadowing by a dense clump; (4) multiple sources in a cosmological density field; (5) classical HII region gasdynamic expansion; (6) HII region gasdynamic expansion in $1/r^2$ density profile, and (7) photoevaporation of a dense clump. The present results and tests represent the most complete benchmark available for the development of new codes and improvement of existing ones. To further this aim all test inputs and outputs are made publicly available in digital form at this website.

Test descriptions, data submission, papers and workshops

Description of the tests and of the required data format for submission.

Submit data here.

The first paper, The Static Density Field Tests: ArXiv,ADS

To date we have organized two workshops related to this comparison project:

First workshop

Second workshop

Data and Results

Static Density Field Tests: Data

Static Density Field Tests: Results

Radiative Hydrodynamic Tests: Data (restricted)

Radiative Hydrodynamic Tests: Results (restricted)

Done

Radiative Transfer Comparison Project Wiki: Data Submission

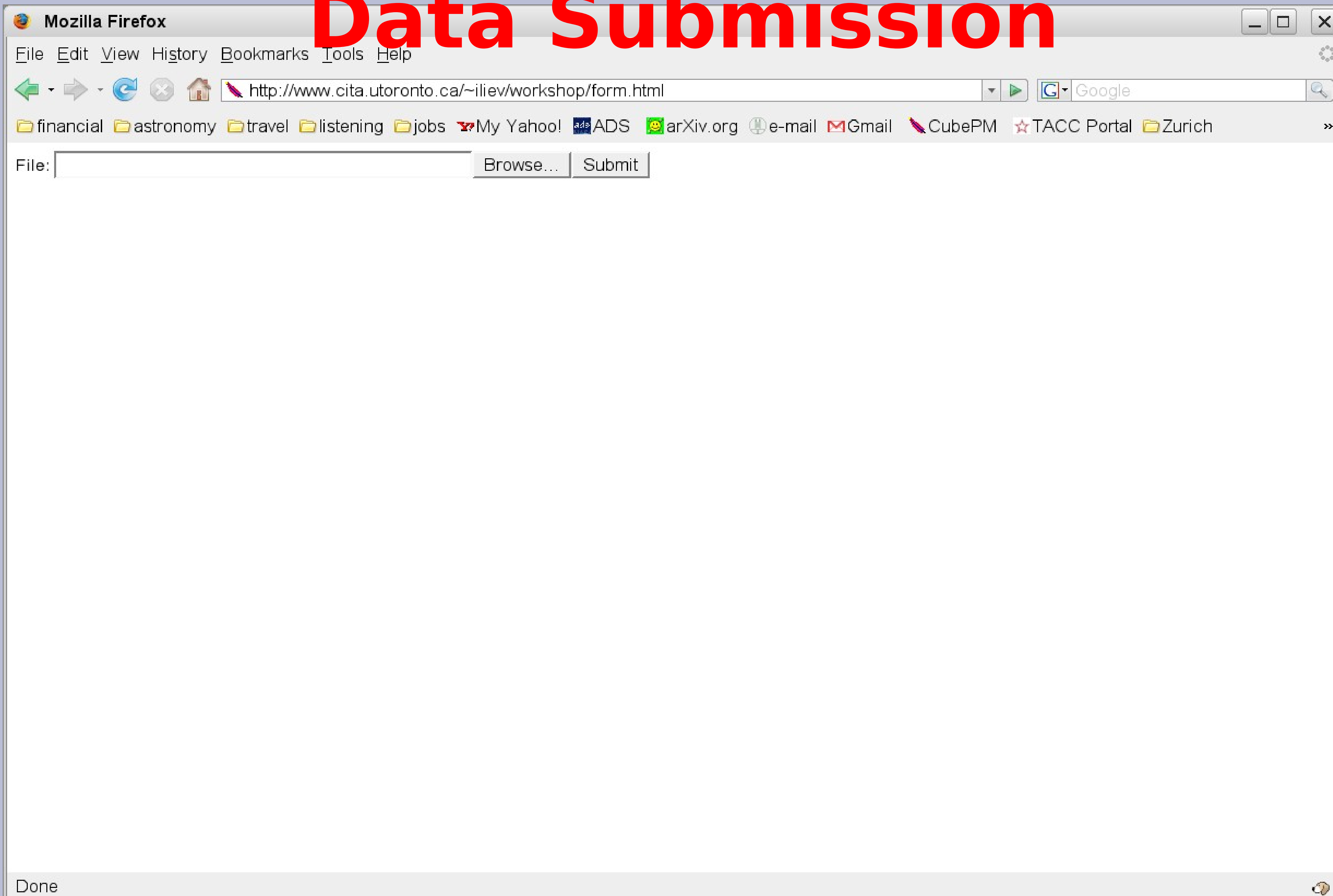

Radiative Transfer Comparison Project Wiki: Results & Errata

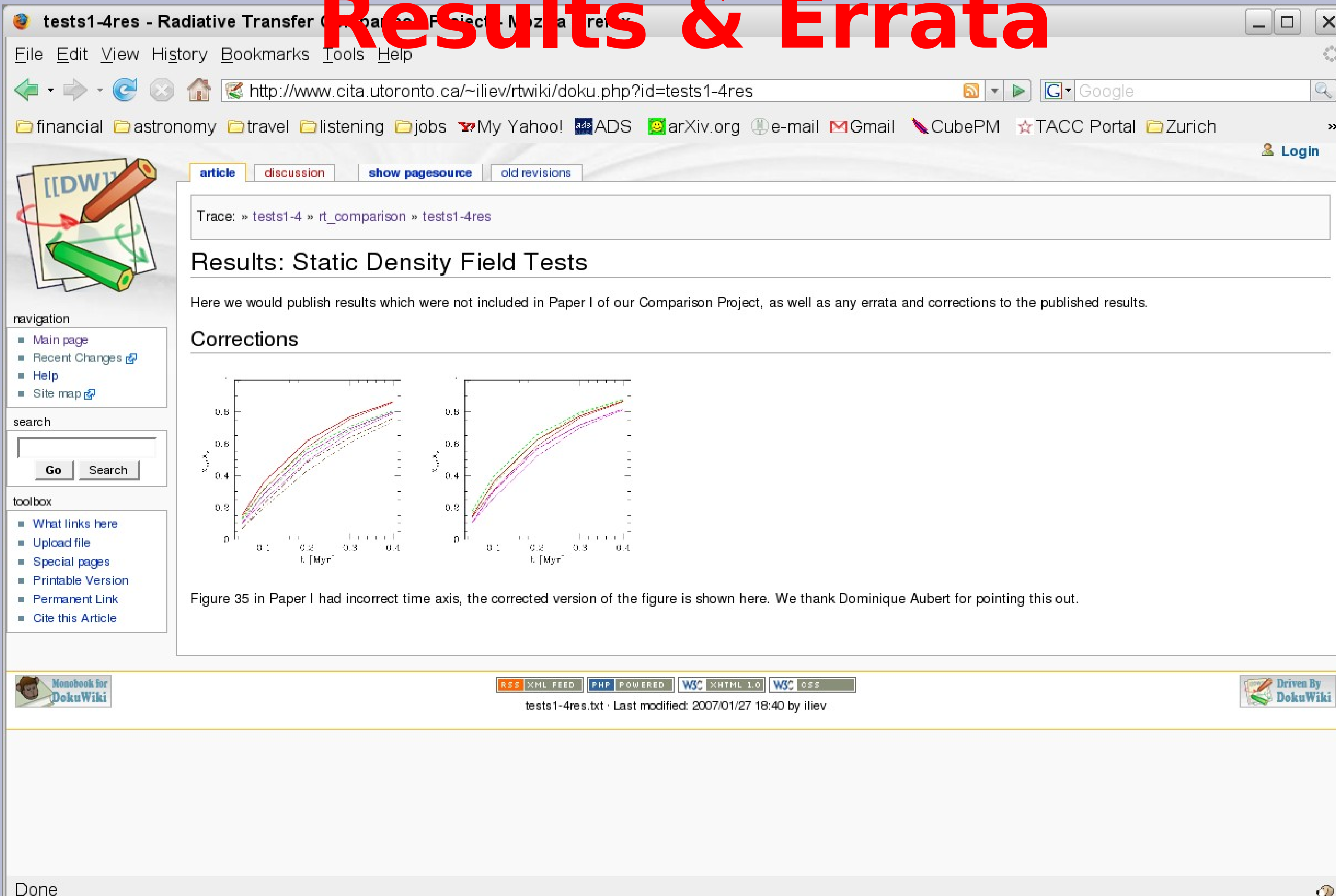

Radiative Transfer Comparison Project Wiki: Results & Errata II

Radiative Transfer Comparison Project Wiki: Data Sharing

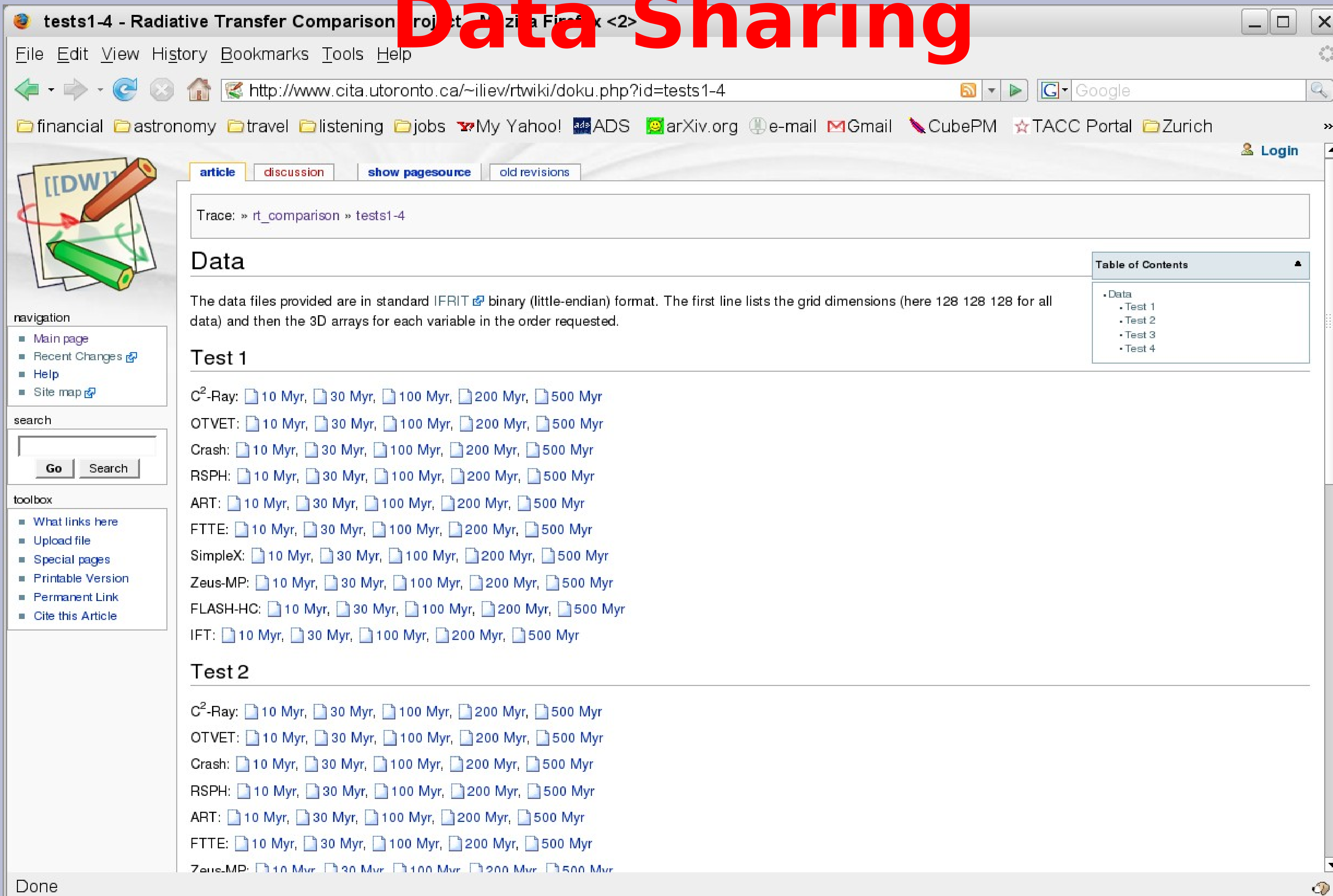

Data Formats

- Maximally simple and machine independent.
- Submission: ASCI data, defined loops and variables order, evolution times at which data is required (typically 5 timeslices, to limit total data amount).
- (Relatively) Low resolution requested (128^3 grid) in interests of inclusivity.
- For standartization data required on a regular grid – not optimal for all codes (e.g. AMR, Lagrangean, unstructured grids).

Issues and problems

- People need regular pushing along, or nothing will happen.
- A number of issues with the data submissions (inevitable when a number of busy people involved?) – significant amount of time and efforts to fix:
  - incorrect data format of submissions (e.g. multiple files instead of one).
  - incorrect variable (e.g. HII instead of HI fraction).
  - different units (e.g. cm vs. kpc, sec vs. Myr).
  - more subtle – in some cases slightly incorrect/different problem ran (e.g. different ionizing spectrum used).

Cosmological Radiative Transfer: specifics

- Main problem: Reionization of the Universe by the first sources.
- Large scales (from kpc to hundreds of Mpc), up to hundreds of thousands of sources.
- Low densities -> fast I-fronts (R-type), converting to D-type in denser regions (halos).
- 3D, inhomogeneous density fields.
- Very high optical depths.
- H+He are most important, but metal cooling also matters at later times.

Tests: 0-7

- Test 0 : Basic physics, rates used + single zone evolution in ionizing up and then recombining

Pure radiative transfer tests:

- Test 1: Pure hydrogen isothermal HII region expansion
- Test 2: HII region expansion: the temperature state (H+He or pure H)
- Test 3: I-front trapping in a dense clump and formation of a shadow (w/point source and plane-parallel flux)
- Test 4: Multiple sources in a (fixed)

Tests: 0-7 (cont.)

Radiative hydrodynamics tests:

- Test 5: Classical HII region expansion and R-type to D-type transition
- Test 6: HII region expansion in $1/r^2$ profile: (re-)acceleration down a steep density profile and inside-out dwarf galaxy photoevaporation
- Test 7: Photoevaporation of a dense clump (w/point source and plane-parallel flux)

Chemistry and Cooling Rates (Test 0)

Chemistry and cooling rates vary significantly between sources in literature – this can introduce noticeable variations in the results.

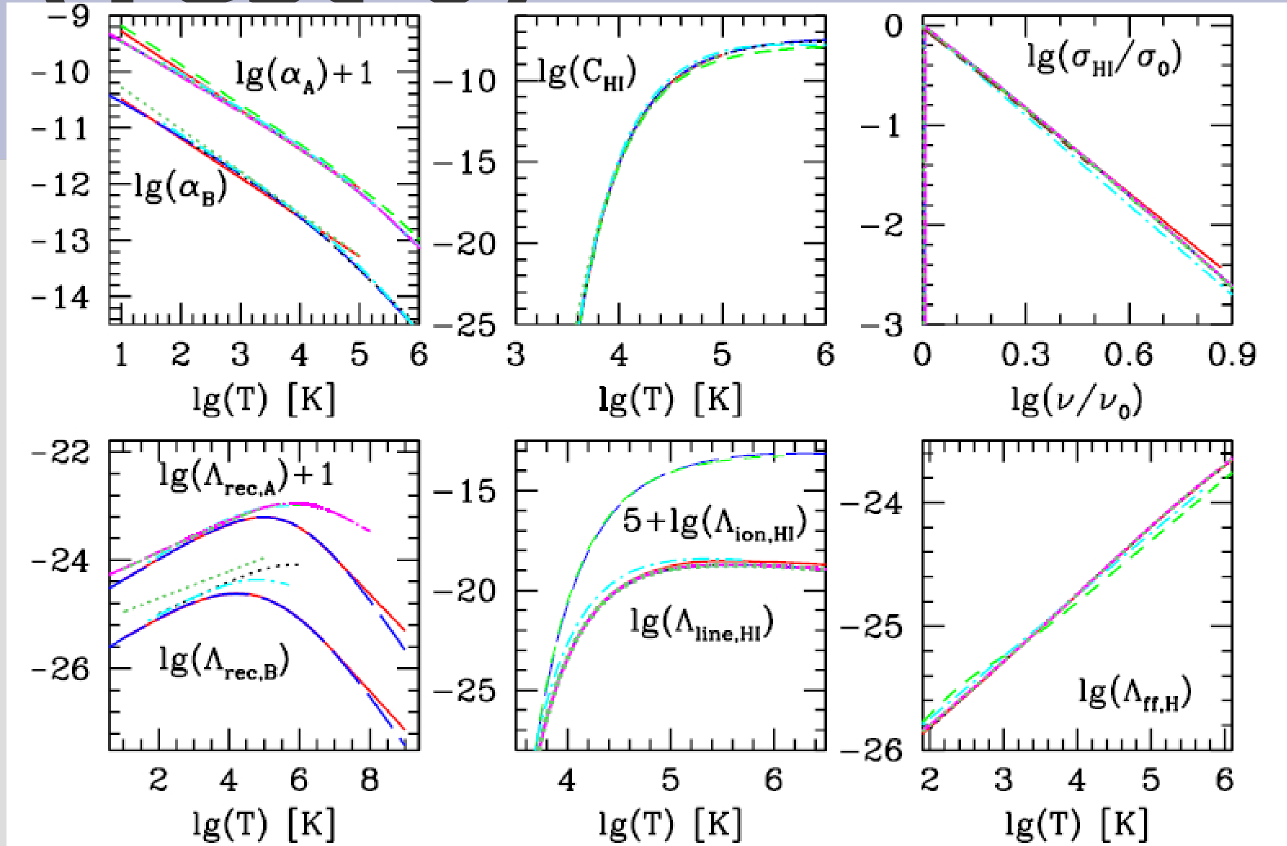

Figure 2. Test 0, part 1: Hydrogen rates, cooling and cross-sections used by the participating codes:
α_B; collisional ionization rate, $C_{\rm HI}$; cross-section, σ_{HI}/σ_0, normalized to the value at the ionizat
case A recombination cooling rate, $\Lambda_{\rm rec,A}$; case B recombination cooling rate, $\Lambda_{\rm rec,B}$; collisional
rate for hydrogen, $\Lambda_{\rm ff,H}$. Units of α_A, α_B, and $C_{\rm HI}$ are [cm^{3}s^{-1}], units of the cooling rates are [

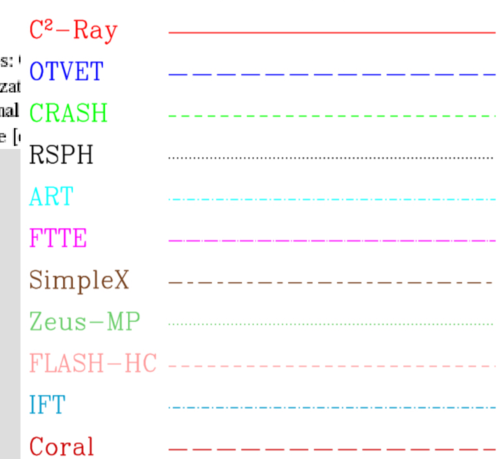

Chemistry and Cooling Rates: effects

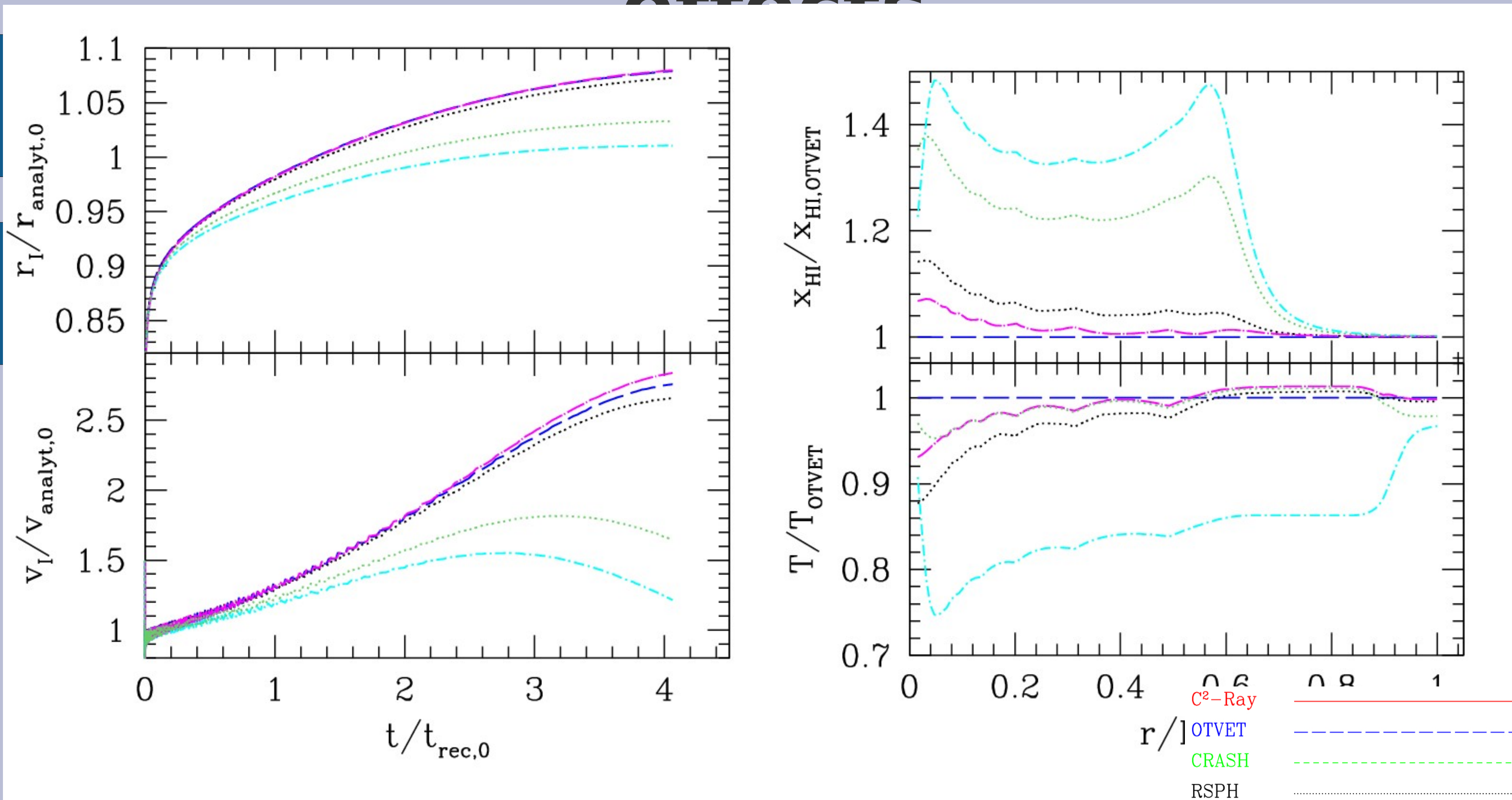

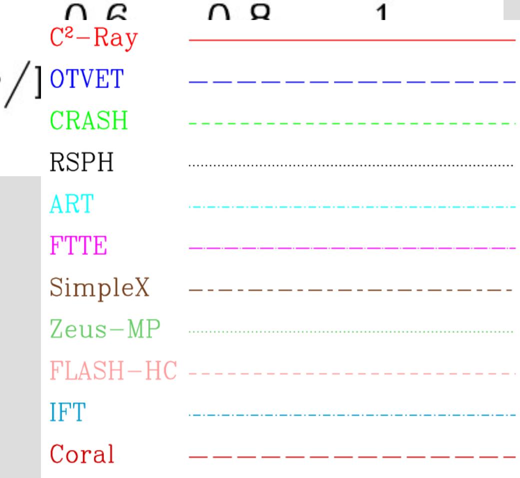

same RT method, different rates

Examples:Test 2: initial expansion

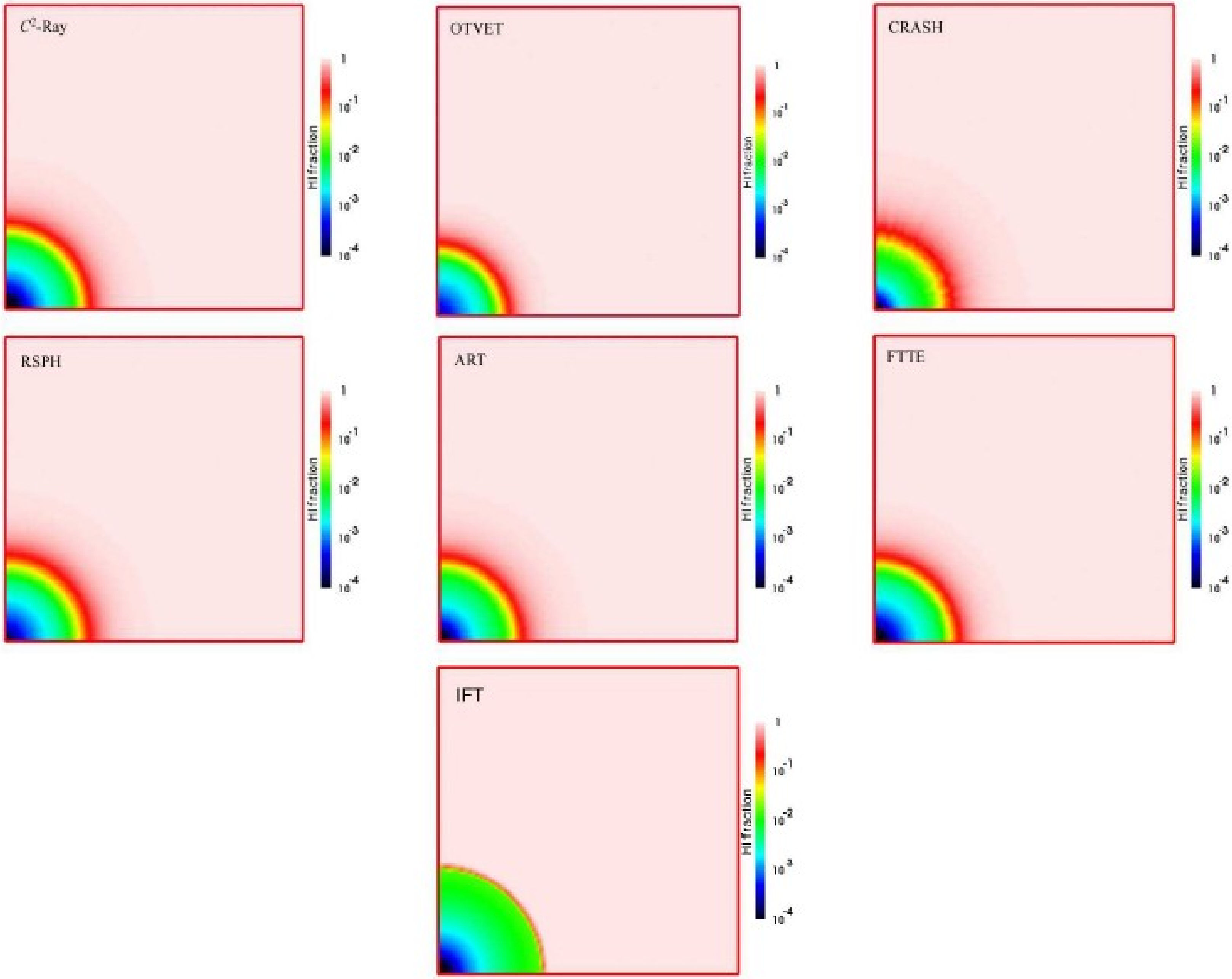

Figure 11. Test 2 (H II region expansion in an uniform gas with varying temperature): Images of the H I fraction, cut through the simulation volume at coordinate $z = 0$ at time $t = 10$ Myr for (left to right and top to bottom) C^2-Ray, OTVET, CRASH, RSPH, ART, FTTE, and IFT.

Test 2: T during initial expansion

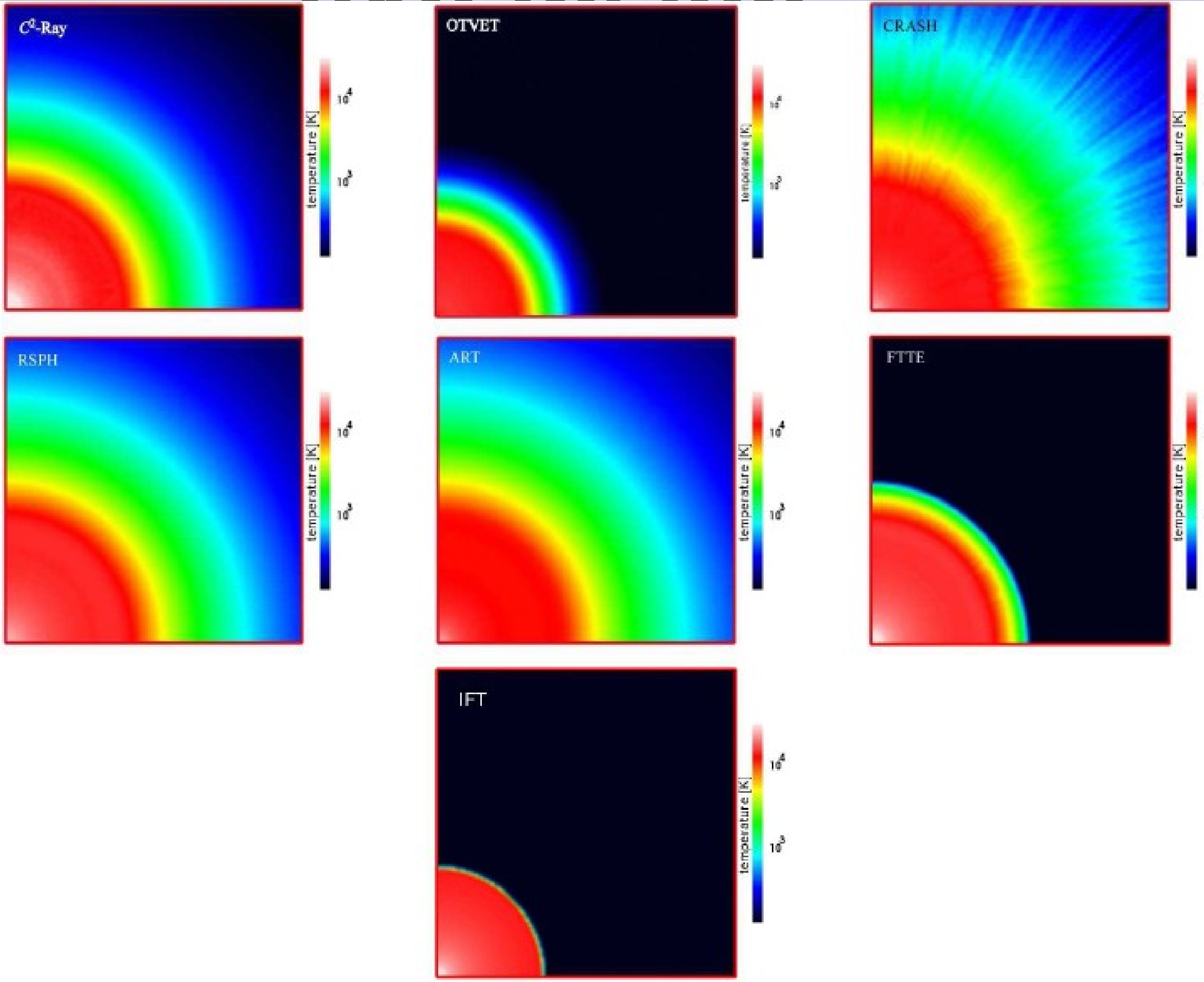

Figure 12. Test 2 (H II region expansion in an uniform gas with varying temperature): Images of the temperature, cut through the simulation volume at coordinate $z = 0$ at time $t = 10$ Myr for (left to right and top to bottom) C^2-Ray, OTVET, CRASH, RSPH, ART, FTTE, and IFT.

Test 2: Stromgren sphere

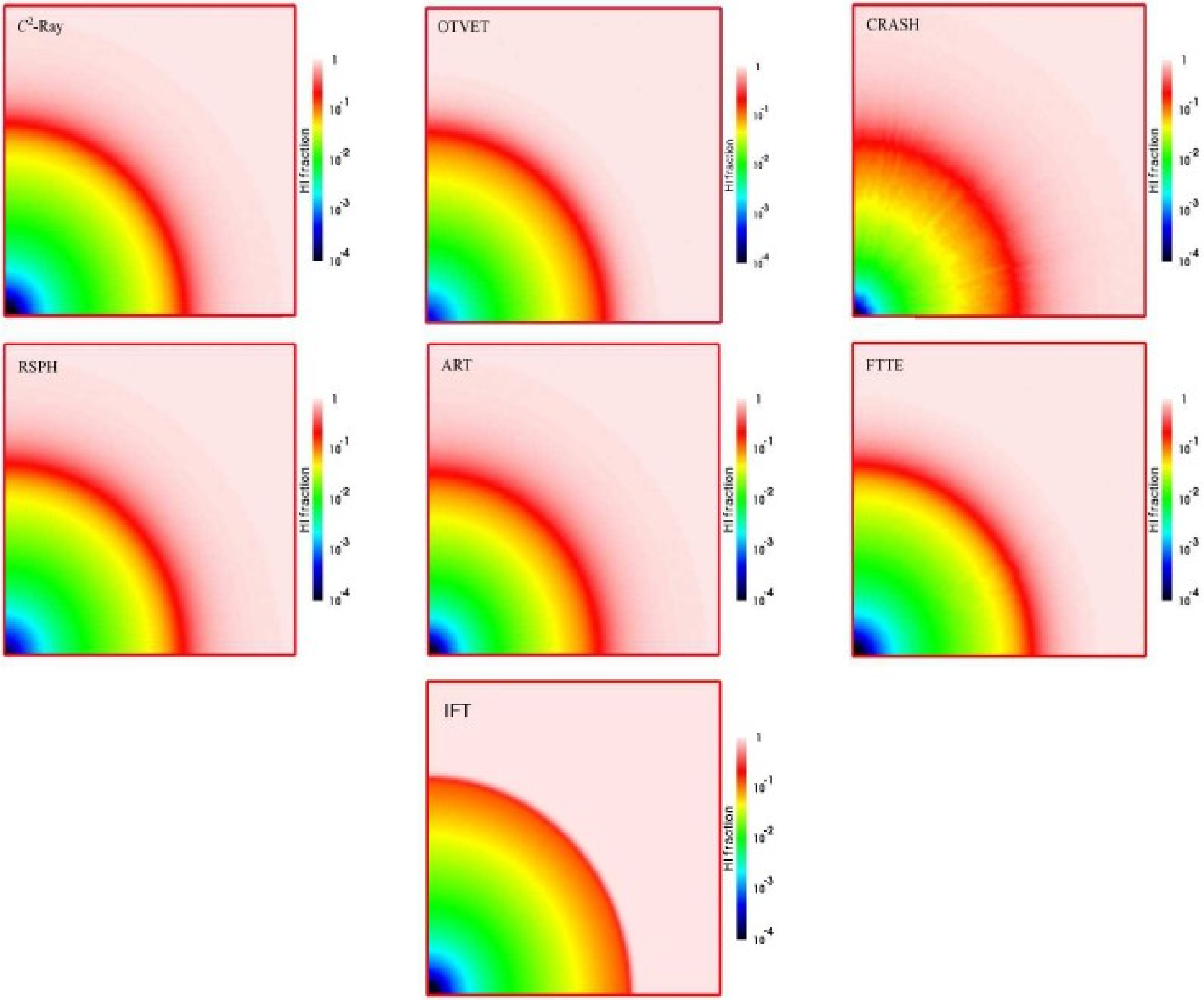

Figure 13. Test 2 (H II region expansion in an uniform gas with varying temperature): Images of the H I fraction, cut through the simulation volume at coordinate $z = 0$ at time $t = 100$ Myr for (left to right and top to bottom) C^2-Ray, OTVET, CRASH, RSPH, ART, FTTE, and IFT.

Test 2: Stromgren sphere T

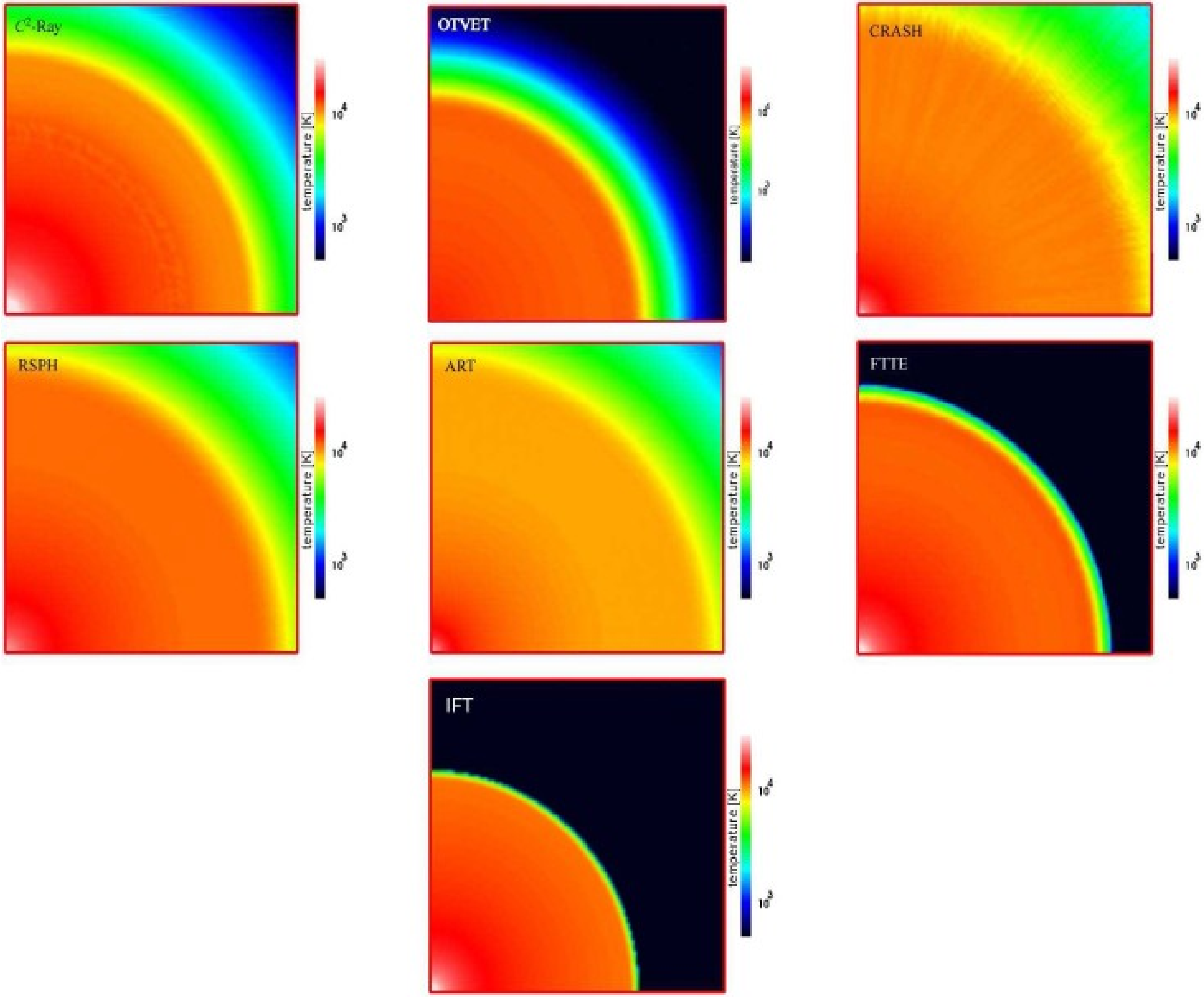

Figure 14. Test 2 (H II region expansion in an uniform gas with varying temperature): Images of the temperature, cut through the simulation volume at coordinate $z = 0$ at time $t = 100$ Myr for (left to right and top to bottom) C^2-Ray, OTVET, CRASH, RSPH, ART, FTTE, and IFT.

Test 2: ionization structure

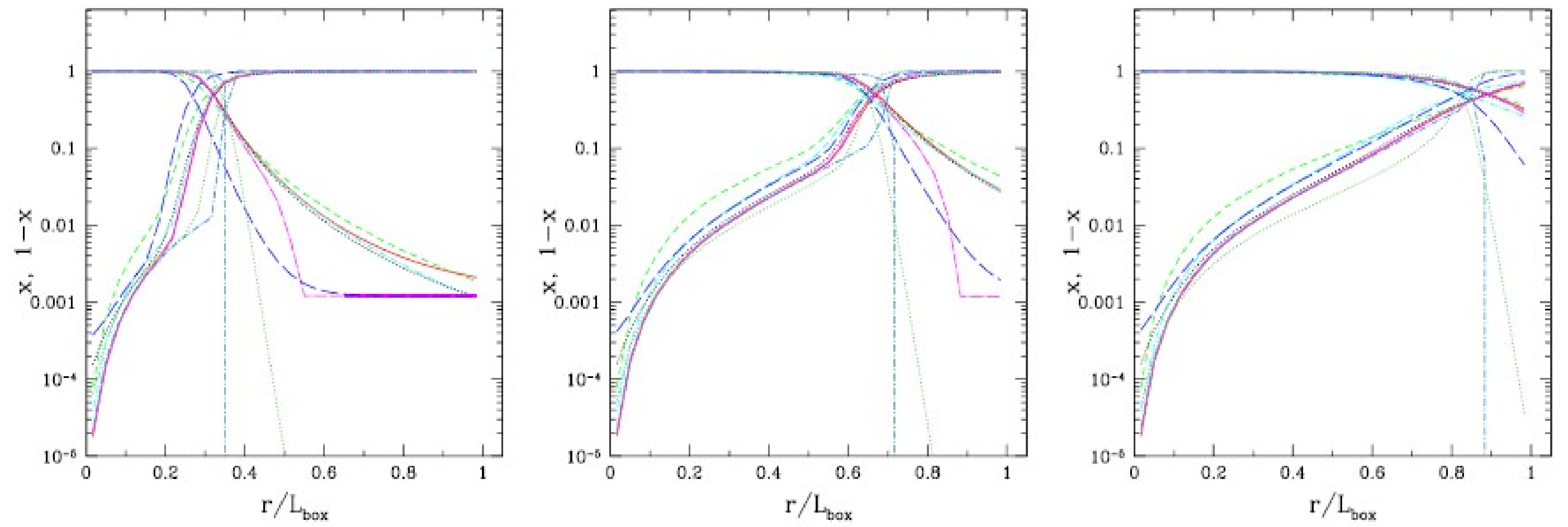

ı gas with varying temperature): Spherically-averaged ionized fraction x and neutral fraction $1-x$

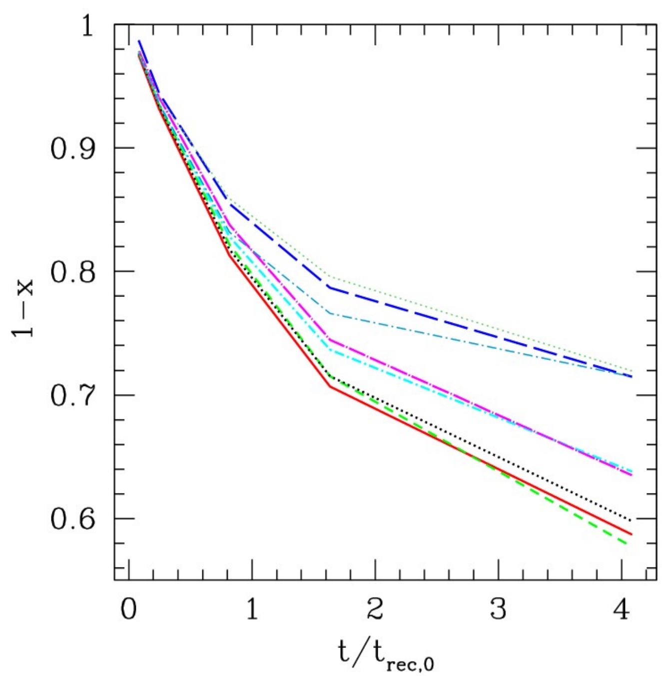

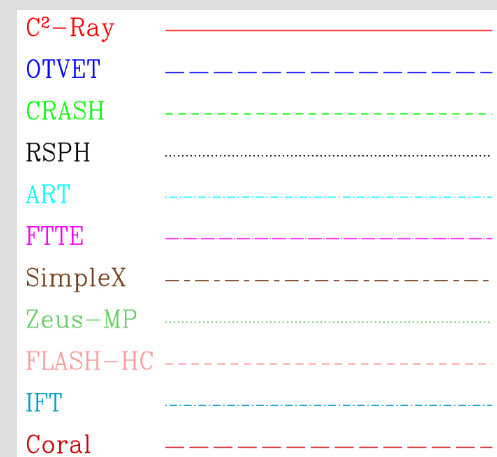

Test 2: temperature structure

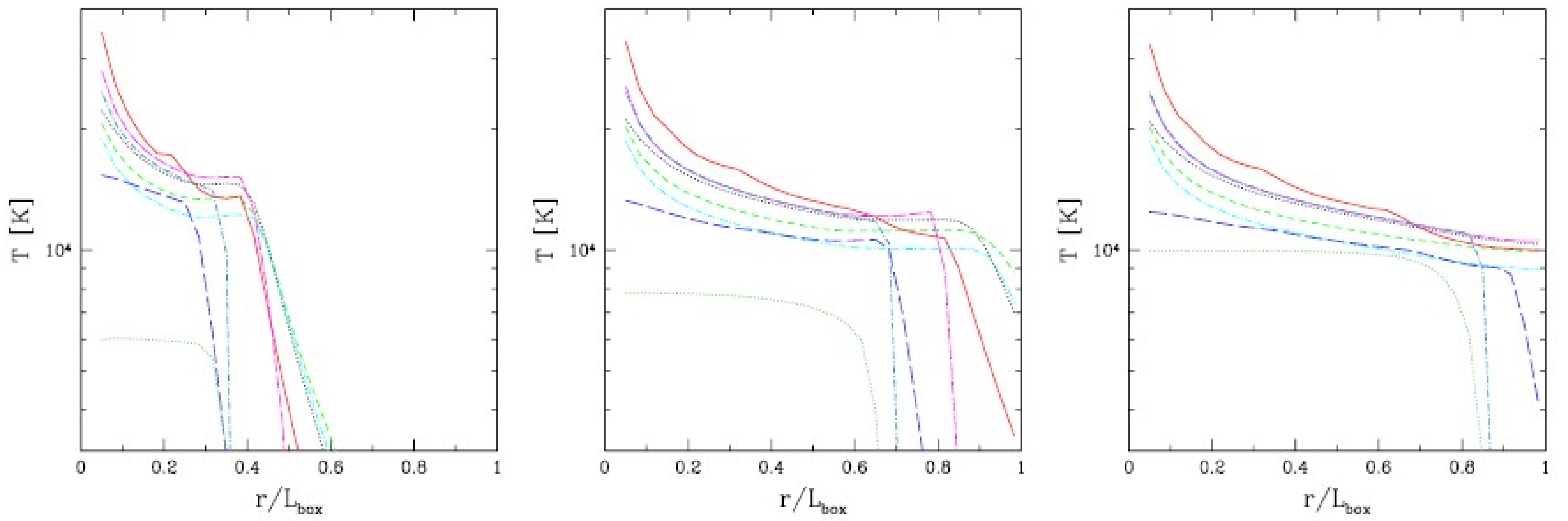

Figure 17. Test 2 (H II region expansion in an uniform gas with varying temperature): Spherically-averaged temperature profiles at times t = 10 Myr, 100 Myr and 500 Myr (from left to right).

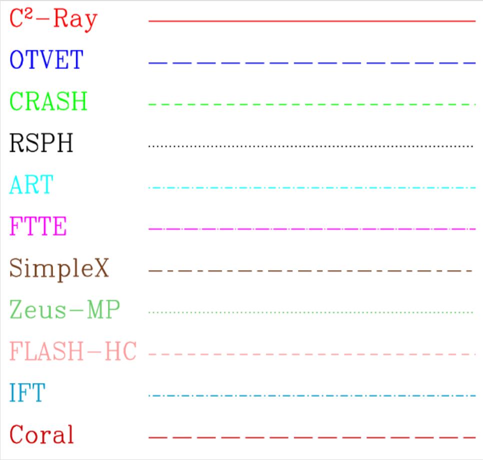

Test 2: x and T histograms

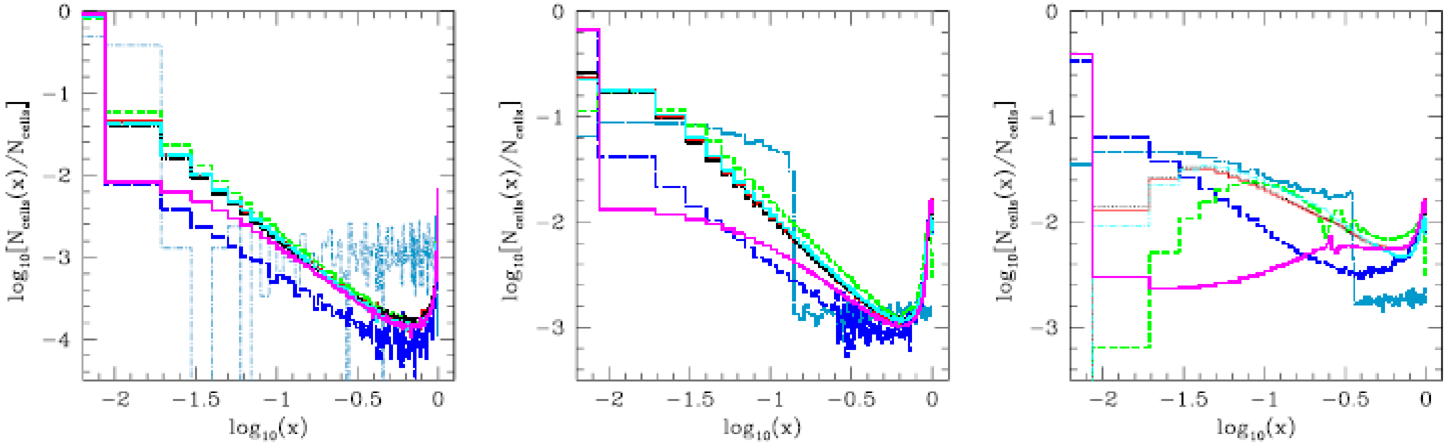

Figure 18. Test 2 (H II region expansion in an uniform gas with varying temperature): Fraction of cells with a given ionized fraction, x, at times (left) $t = 10$ Myr, (middle) 100 Myr and (right) 500 Myr.

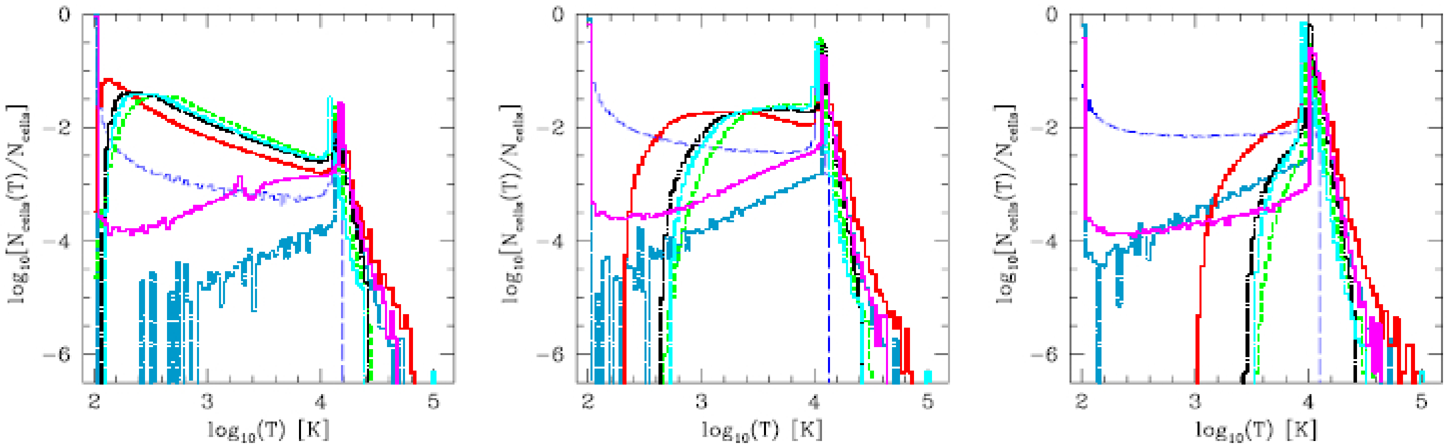

Figure 19. Test 2 (H II region expansion in an uniform gas with varying temperature): Fraction of cells with a given temperature T at times (left) $t = 10$ Myr, (middle) 100 Myr and (right) 500 Myr.

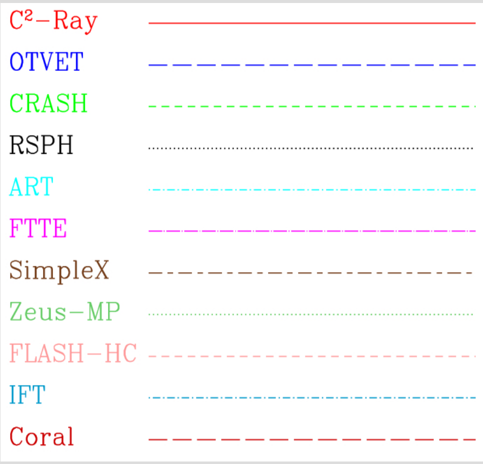

Test 5: the R-type phase

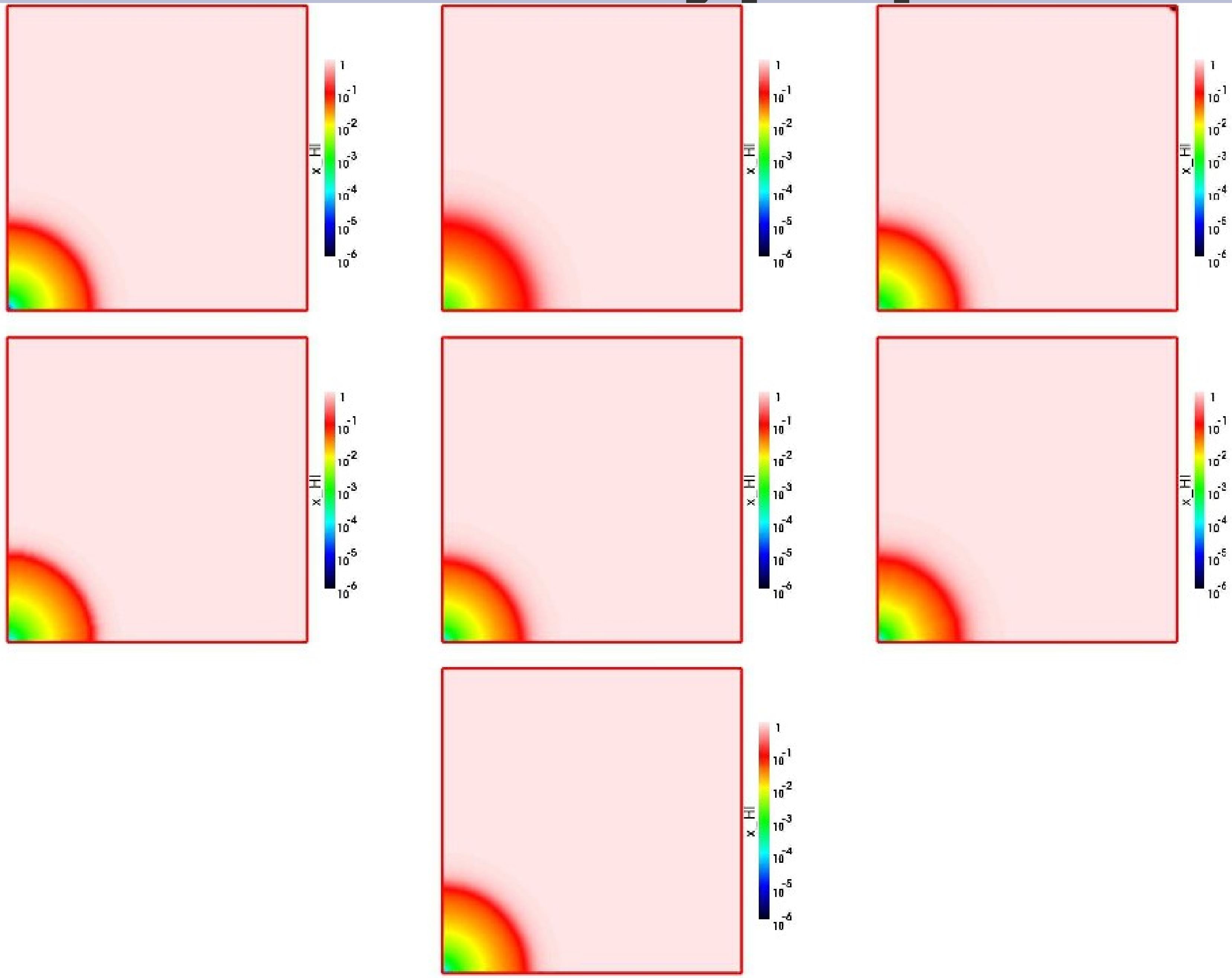

Figure 2. Test 5 (H II region expansion in an initially-uniform gas): Images of the H I fraction, cut through the simulation volume at coordinate $z = 0$ at time $t = 100$ Myr for (left to right and top to bottom) C^2-Ray, HART, RSPH, ZEUS-MP, RH1D, LICORICE, and FLASH.

Test 5: the R-type phase, the pressure

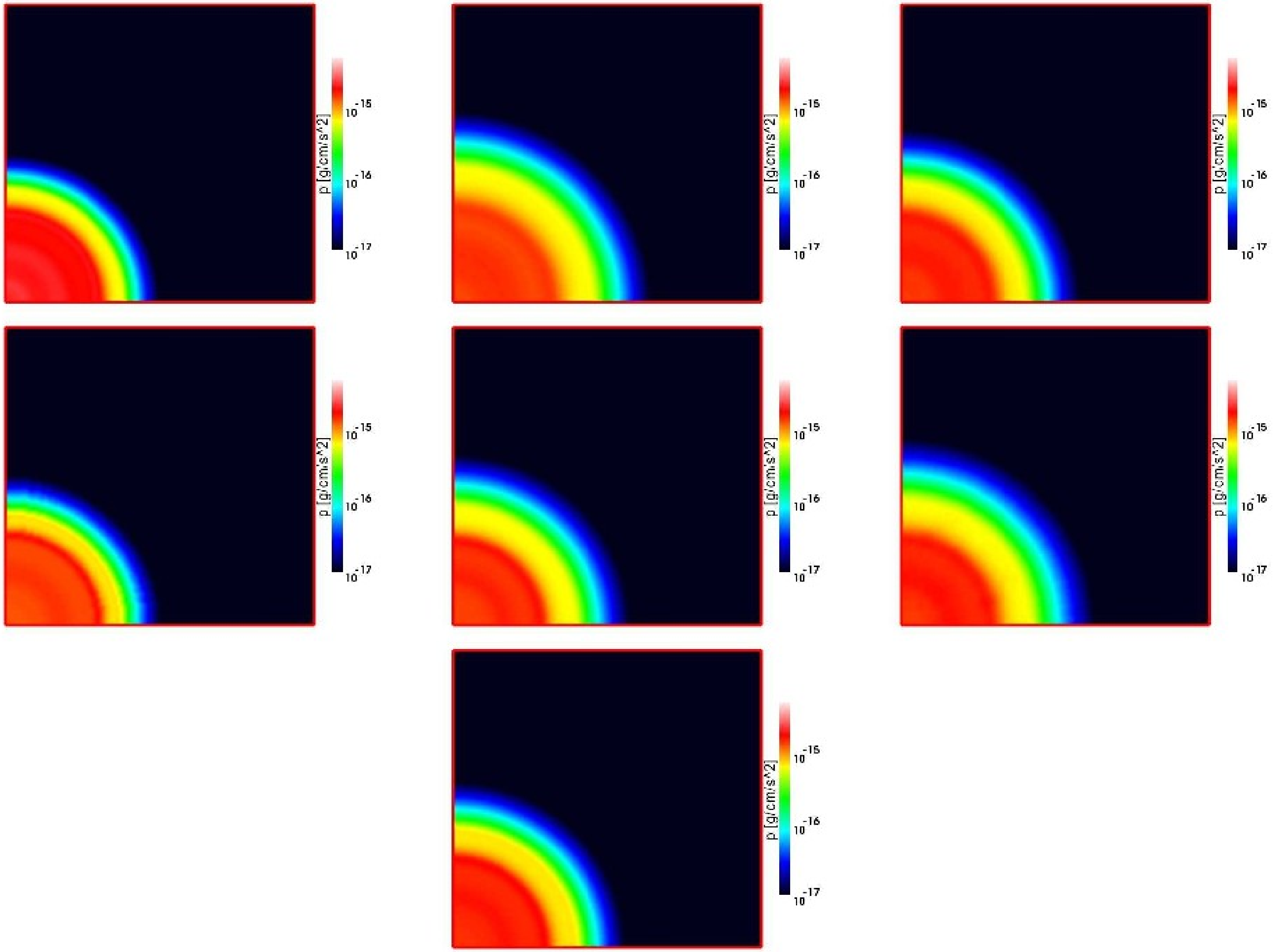

Figure 3. Test 5 (H II region expansion in an initially-uniform gas): Images of the pressure, cut through the simulation volume at coordinate $z = 0$ at time $t = 100$ Myr for (left to right and top to bottom) C^2-Ray, HART, RSPH, ZEUS-MP, RH1D, LICORICE, and FLASH.

Test 5: the R-type phase, the temperature

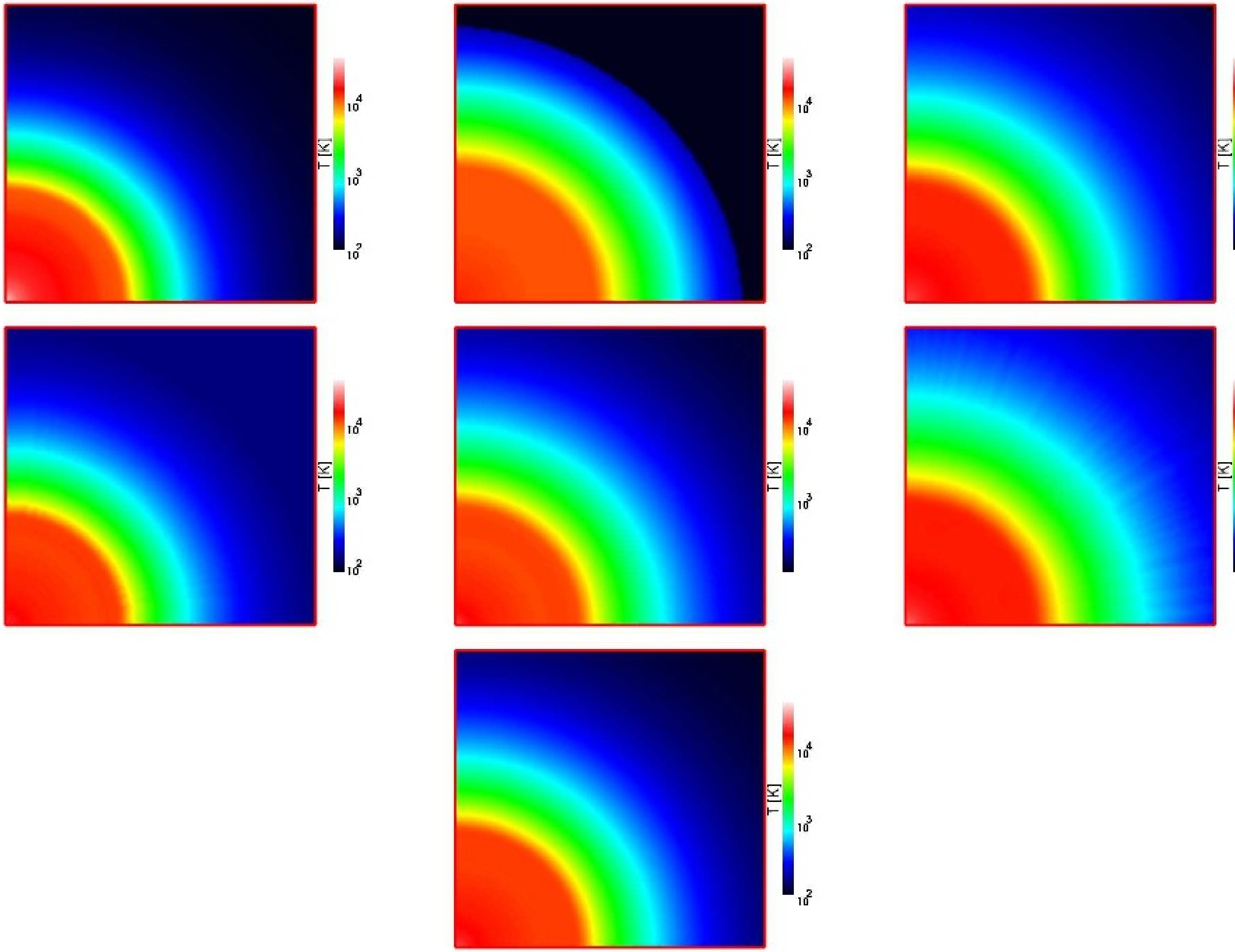

Figure 4. Test 5 (H II region expansion in an initially-uniform gas): Images of the temperature, cut through the simulation volume at coordinate $z = 0$ at time $t = 100$ Myr for (left to right and top to bottom) C^2-Ray, HART, RSPH, ZEUS-MP, RH1D, LICORICE, and FLASH.

Test 5: the D-type phase ion. structure

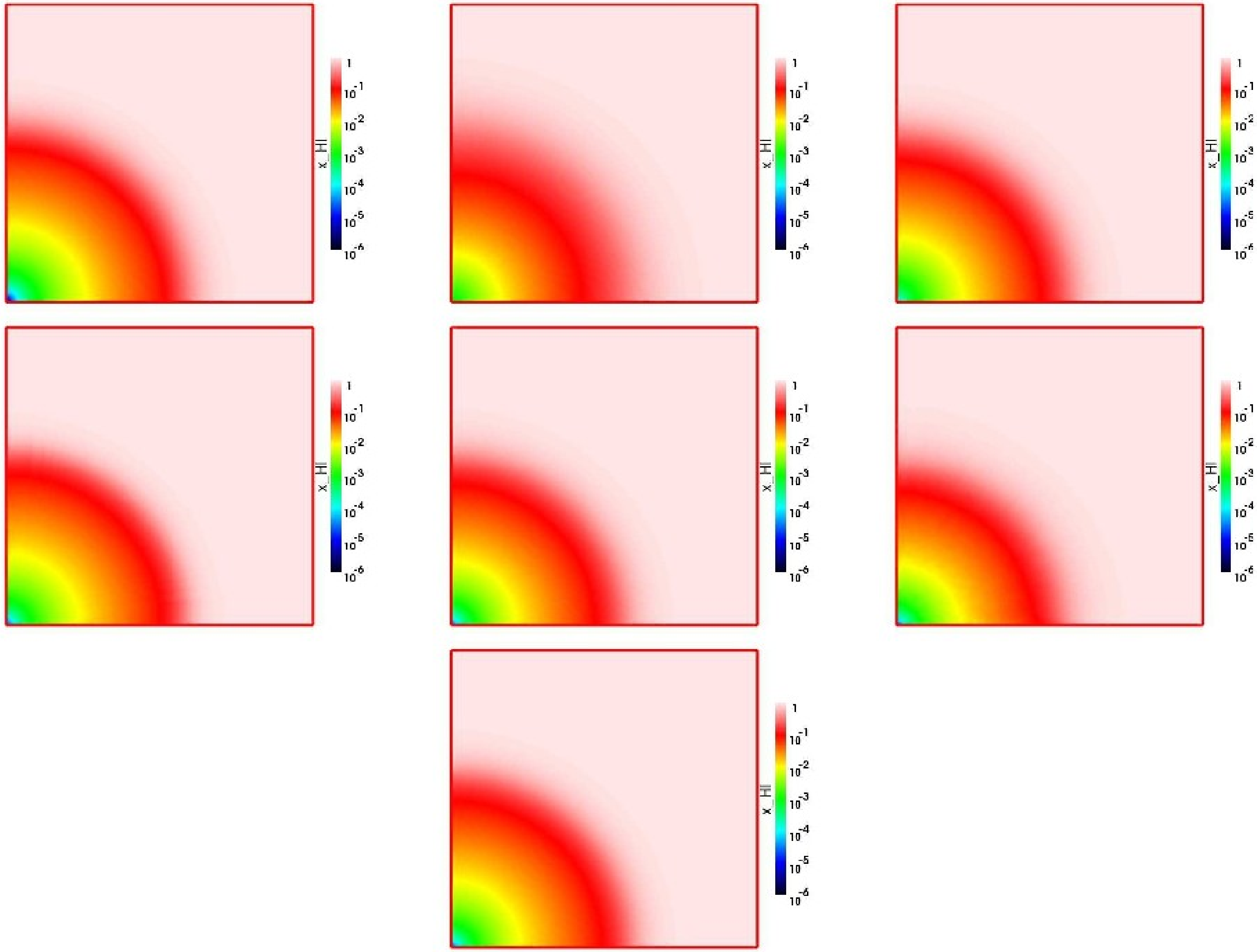

Figure 5. Test 5 (H II region expansion in an initially-uniform gas): Images of the H I fraction, cut through the simulation volume at coordinate $z = 0$ at time $t = 500$ Myr for (left to right and top to bottom) C^2-Ray, HART, RSPH, ZEUS-MP, RH1D, LICORICE, and FLASH.

Test 5: the D-type phase, pressure

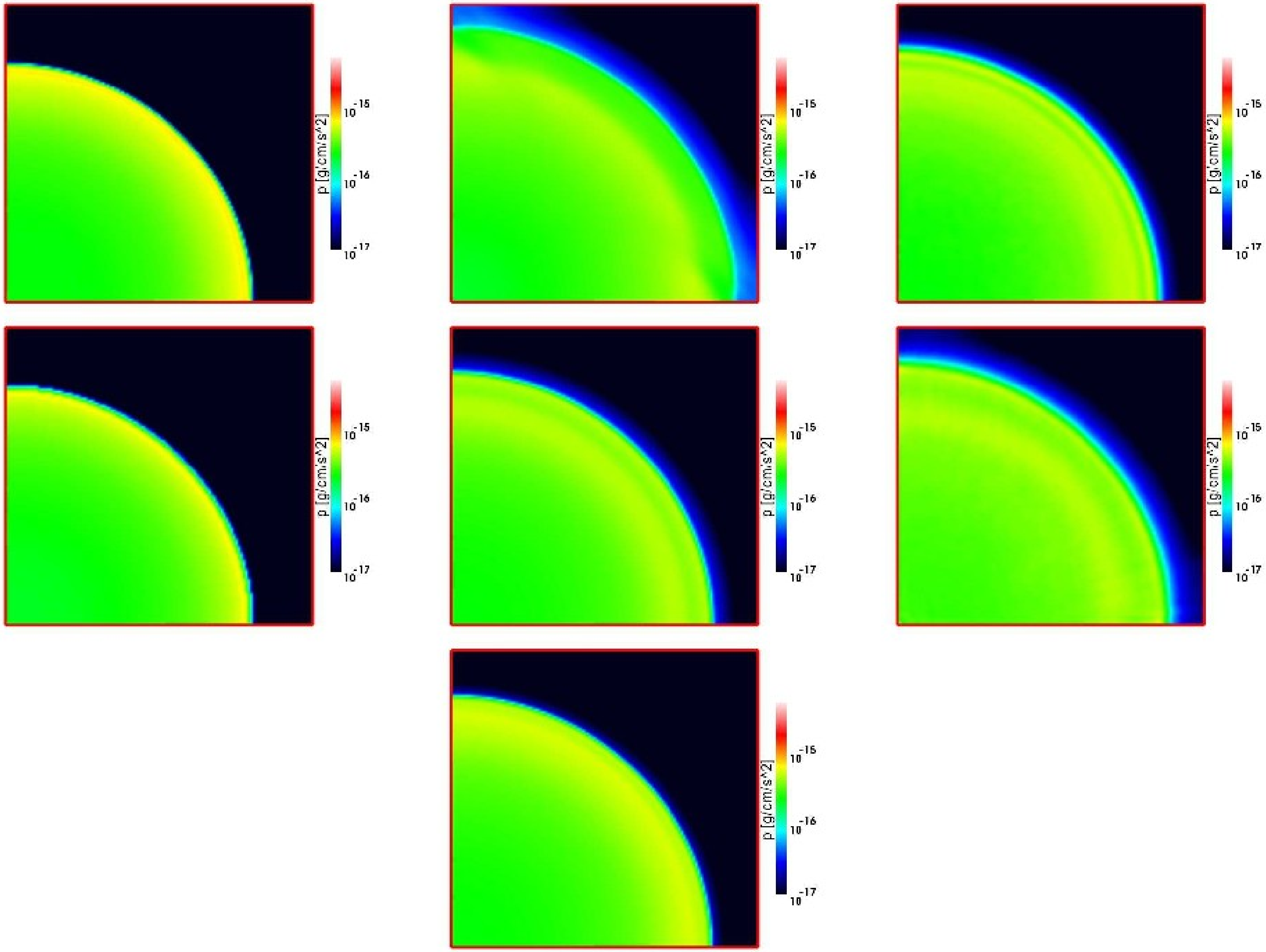

Figure 6. Test 5 (H II region expansion in an initially-uniform gas): Images of the pressure, cut through the simulation volume at coordinate $z = 0$ at time $t = 500$ Myr for (left to right and top to bottom) C^2-Ray, HART, RSPH, ZEUS-MP, RH1D, LICORICE, and FLASH.

Test 5: the D-type phase ion. structure

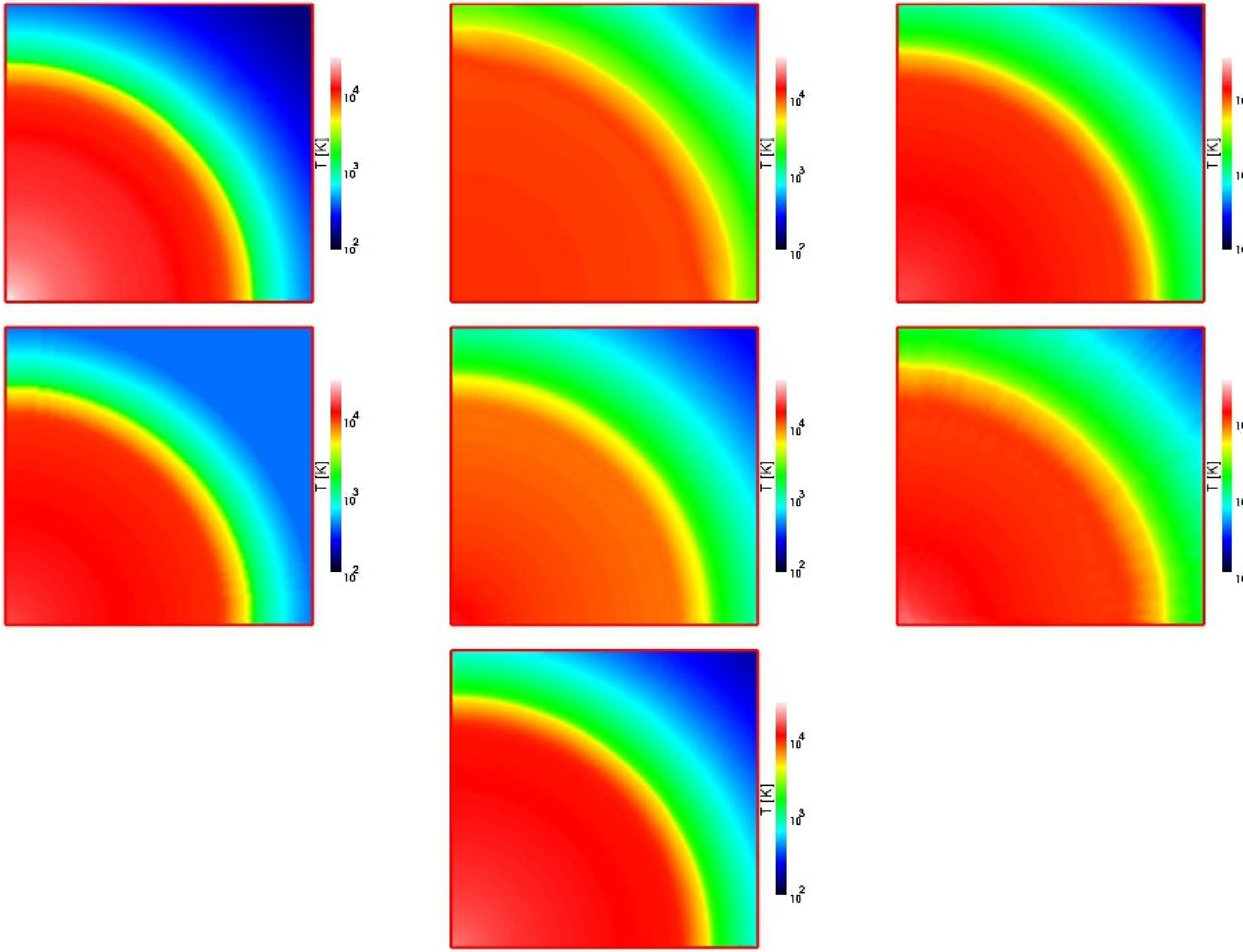

Figure 7. Test 5 (H II region expansion in an initially-uniform gas): Images of the temperature, cut through the simulation volume at coordinate $z = 0$ at time $t = 500$ Myr for (left to right and top to bottom) C^2-Ray, HART, RSPH, ZEUS-MP, RH1D, LICORICE, and FLASH.

Test 5: the D-type phase ion. structure

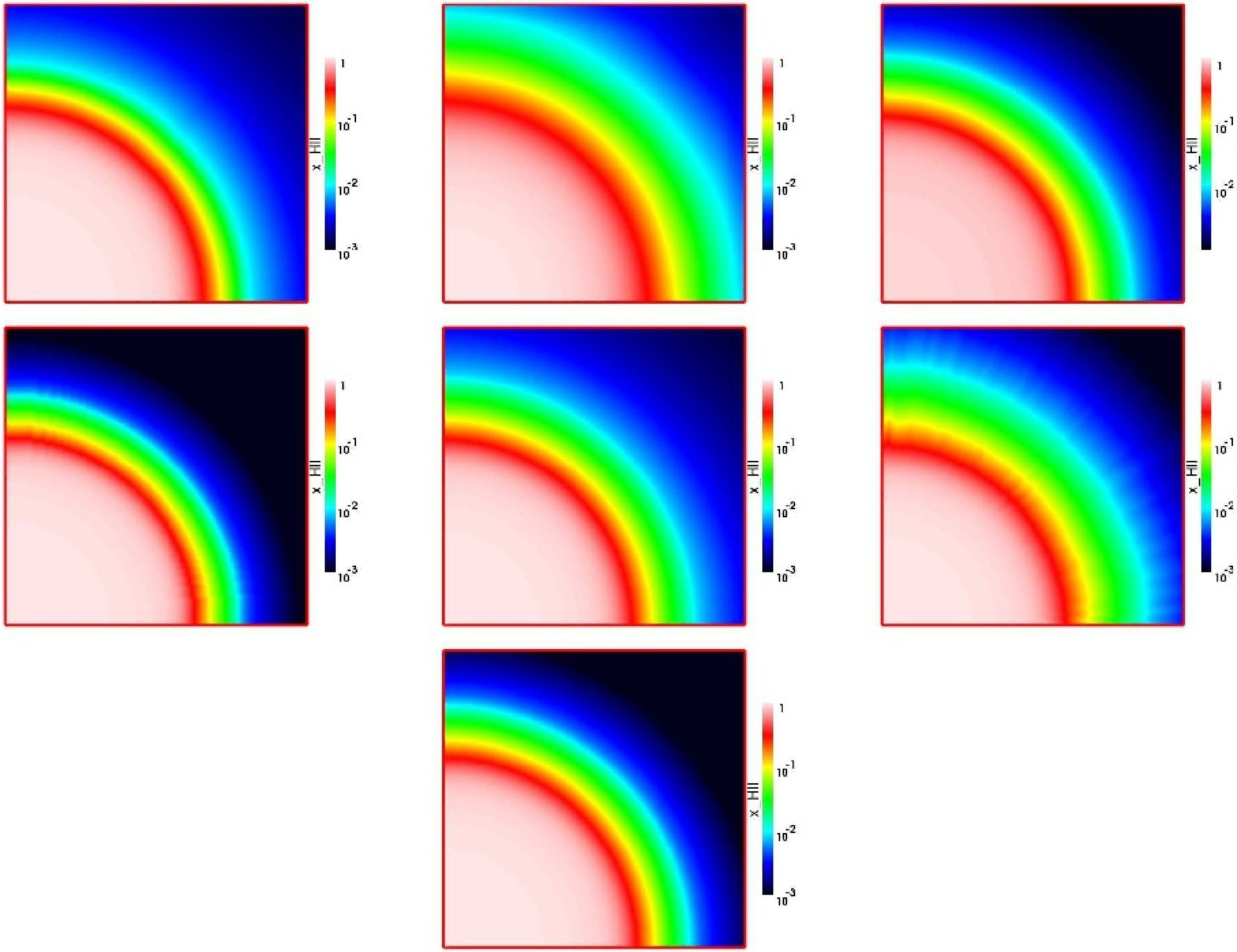

Figure 8. Test 5 (H II region expansion in an initially-uniform gas): Images of the H II fraction, cut through the simulation volume at coordinate $z = 0$ at time $t = 500$ Myr for (left to right and top to bottom) C^2-Ray, HART, RSPH, ZEUS-MP, RH1D, LICORICE, and FLASH.

Test 5: the D-type phase, density

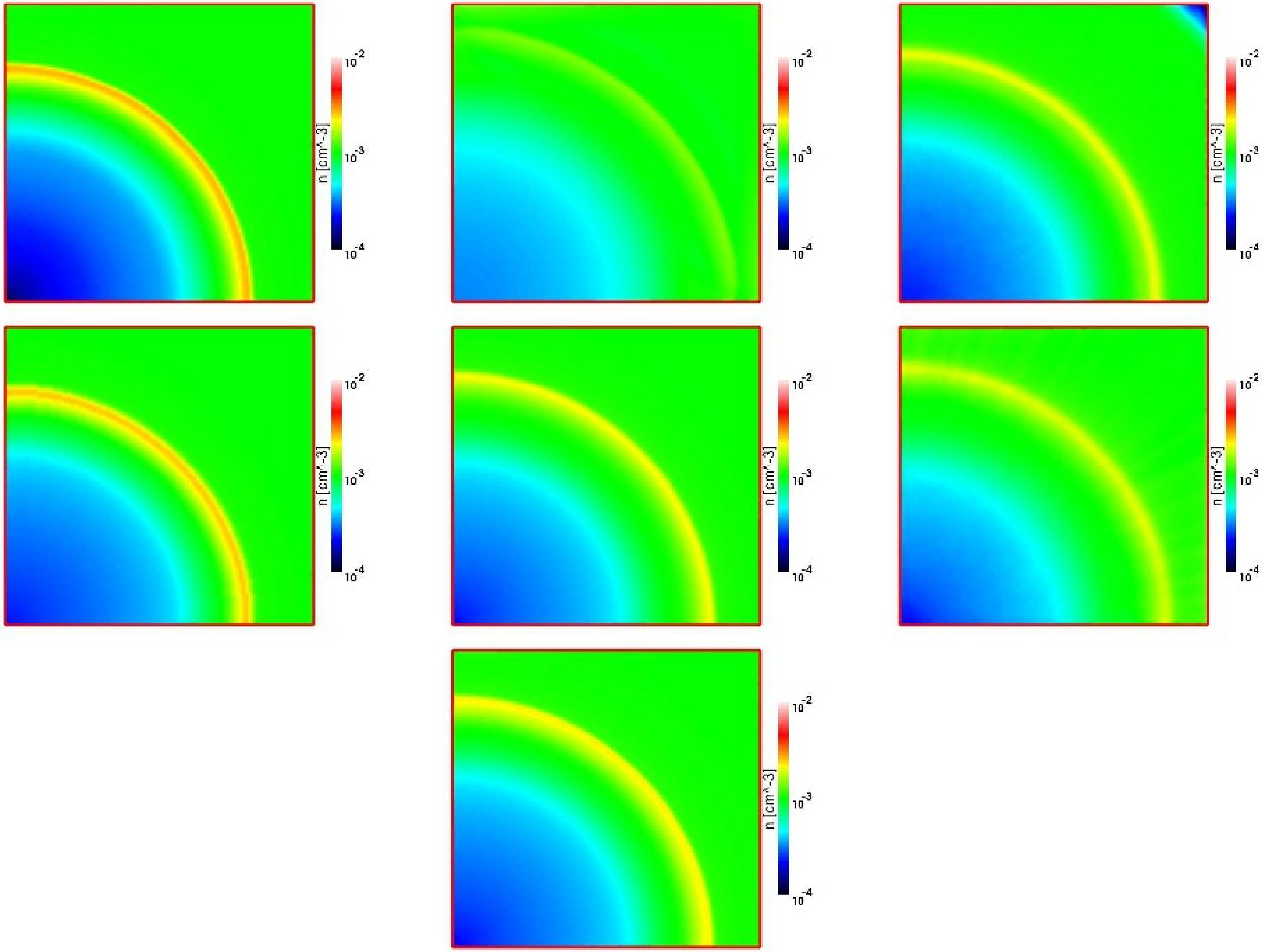

Figure 9. Test 5 (H II region expansion in an initially-uniform gas): Images of the gas number density, cut through the simulation volume at coordinate $z = 0$ at time $t = 500$ Myr for (left to right and top to bottom) C^2-Ray, HART, RSPH, ZEUS-MP, RH1D, LICORICE, and FLASH.

Test 5: the D-type phase, mach

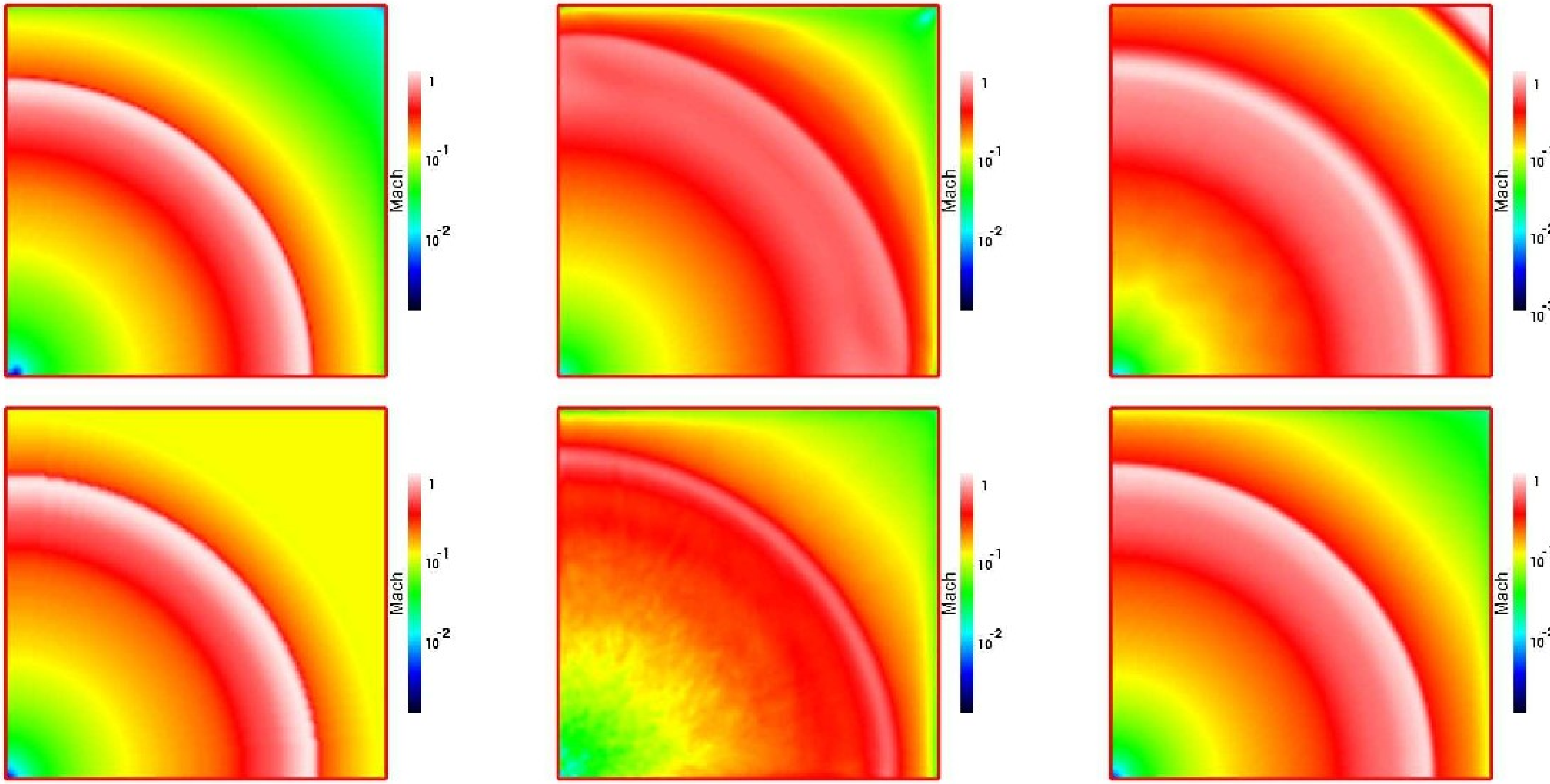

Figure 10. Test 5 (H II region expansion in an initially-uniform gas): Images of the Mach number, cut through the simulation volume at coordinate $z = 0$ at time $t = 500$ Myr for (left to right and top to bottom) C^2-Ray, HART, RSPH, ZEUS-MP, LICORICE, and FLASH.

Test 5: I-front position and velocity

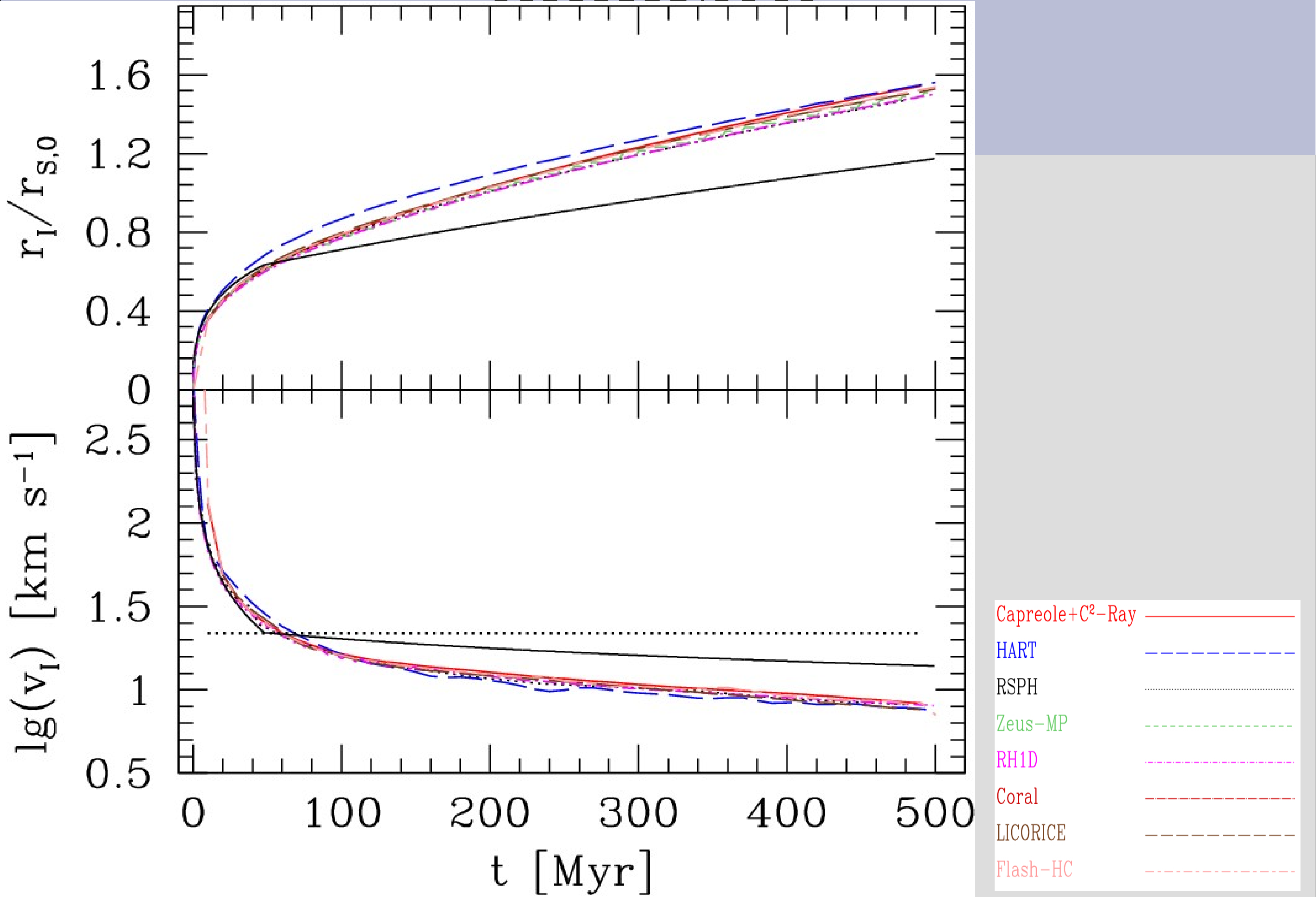

Test 5: Ionization & density structure

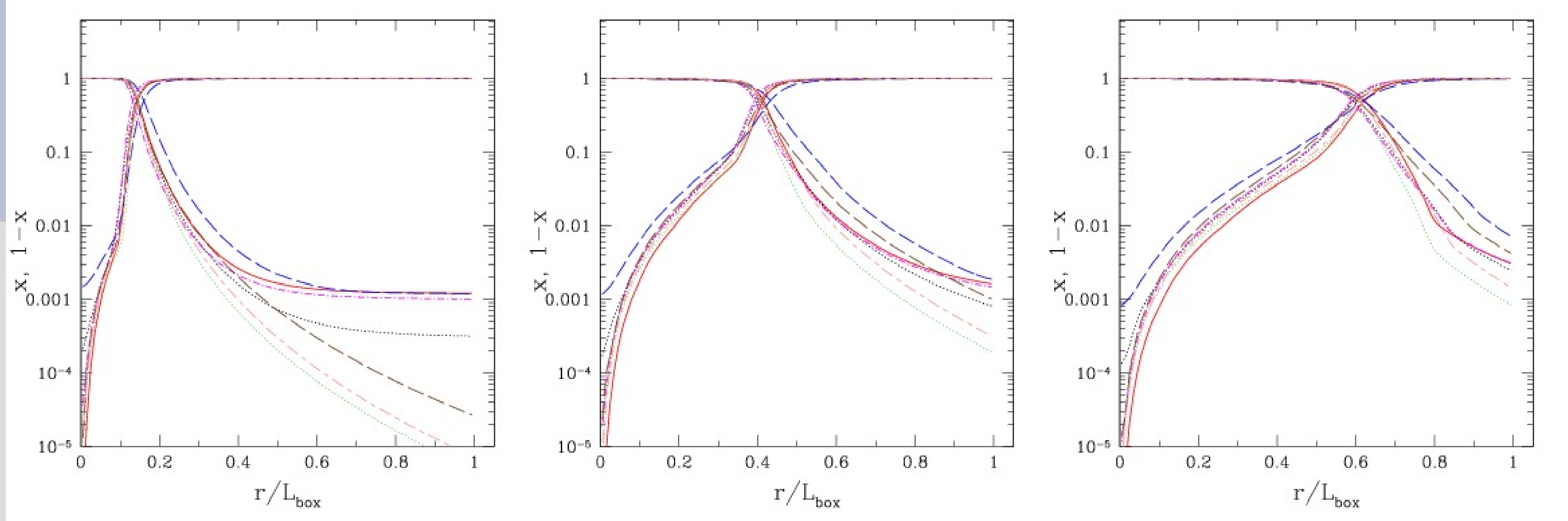

Figure 11. Test 5 (H II region expansion in an initially-uniform gas): Spherically-averaged profiles for ionized fractions x and neutral fractions $x_{\rm xhi} = 1 - x$ at times $t = 10$ Myr, 200 Myr and 500 Myr vs. dimensionless radius (in units of the box size).

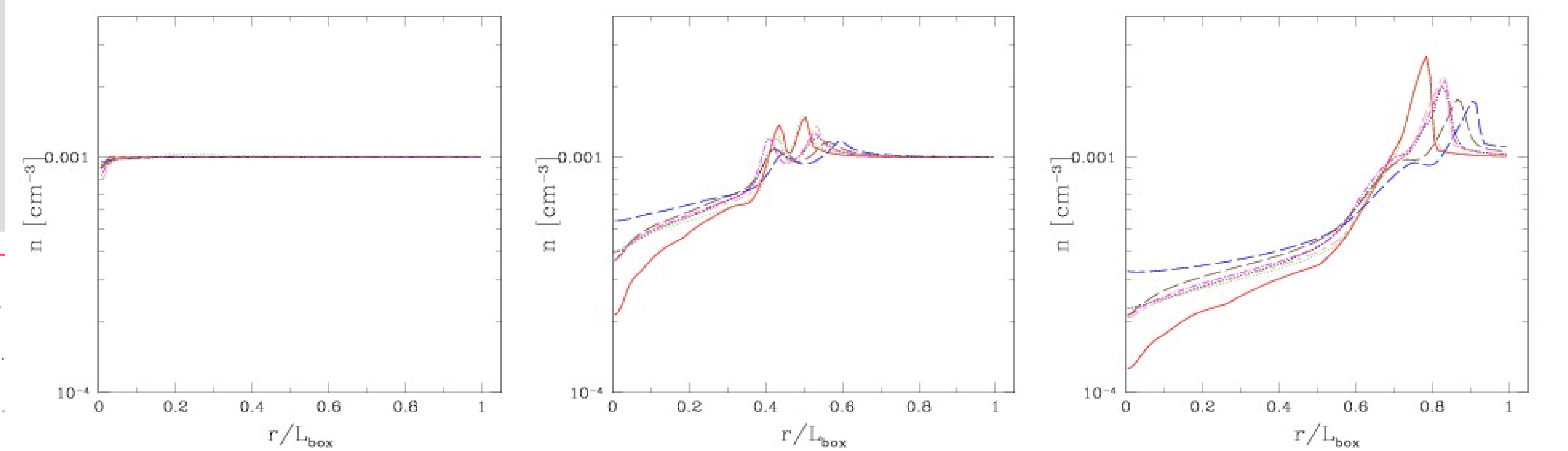

Figure 14. Test 5 (H II region expansion in an initially-uniform gas): Spherically-averaged profiles for the hydrogen number density, n, at times $t = 10$ Myr, 200 Myr and 500 Myr vs. dimensionless radius (in units of the box size).

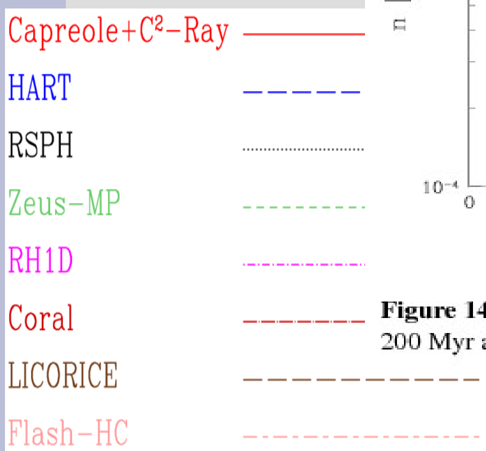

Test 5: pressure & temp. structure

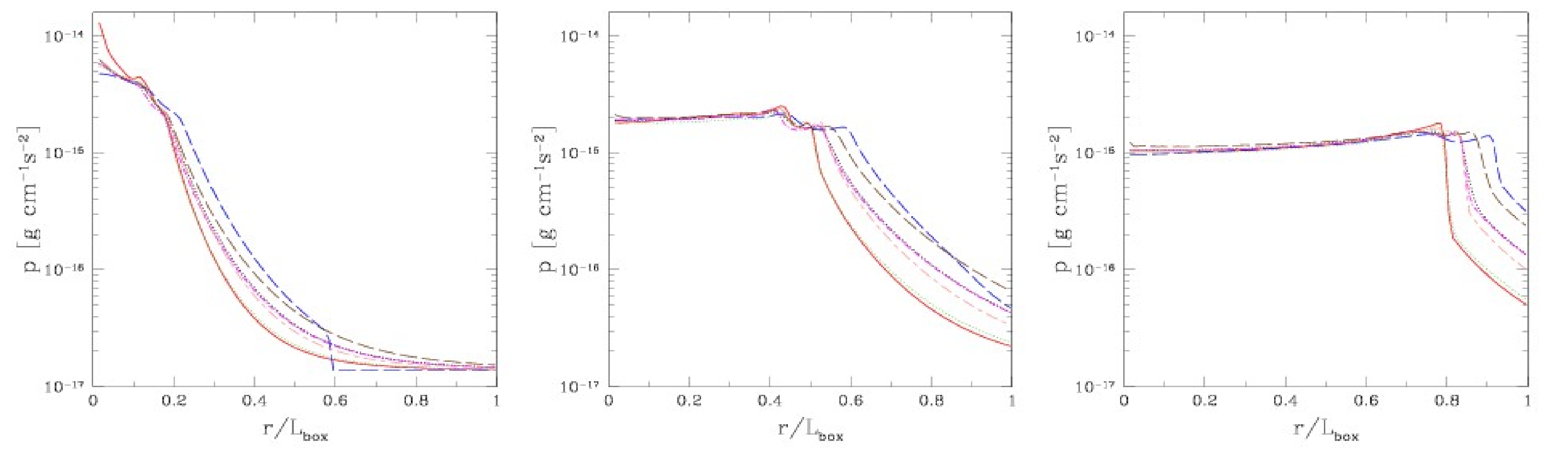

Figure 12. Test 5 (H II region expansion in an initially-uniform gas): Spherically-averaged profiles for pressure, p, at times t = 10 Myr, 200 Myr and 500 Myr vs. dimensionless radius (in units of the box size).

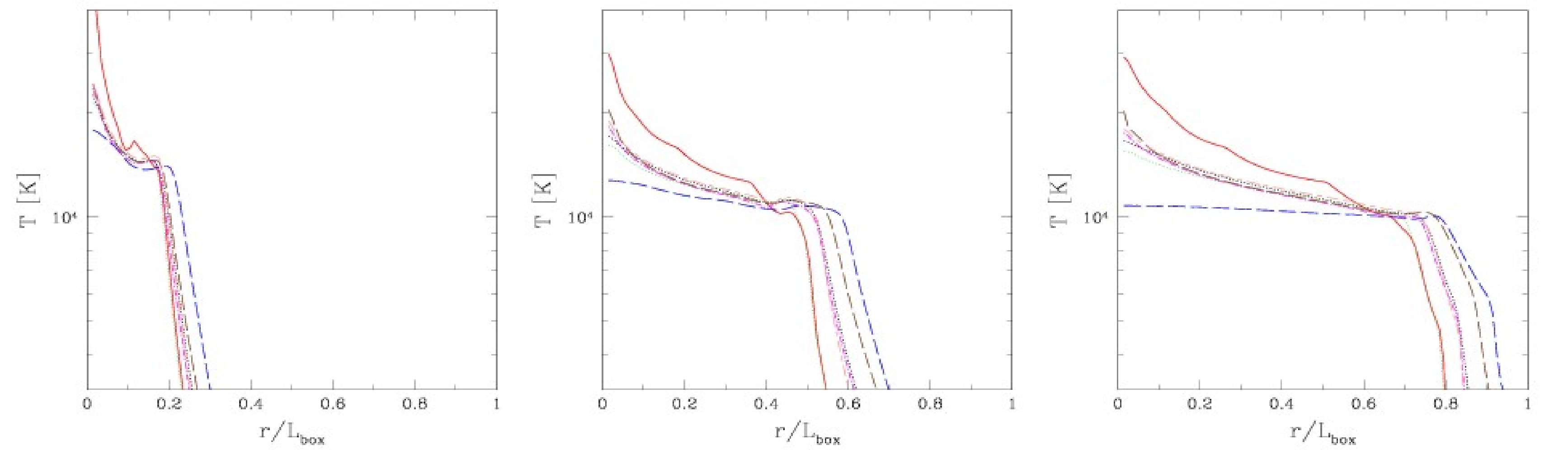

Figure 13. Test 5 (H II region expansion in an initially-uniform gas): Spherically-averaged profiles for temperature at times t = 10 Myr, 200 Myr and 500 Myr vs. dimensionless radius (in units of the box size).

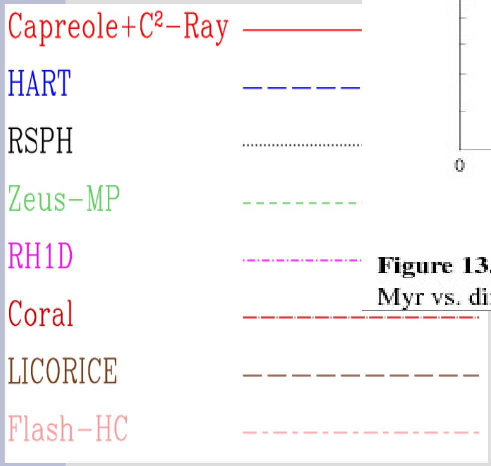

Test 6: the accelereting phase, ion. structure

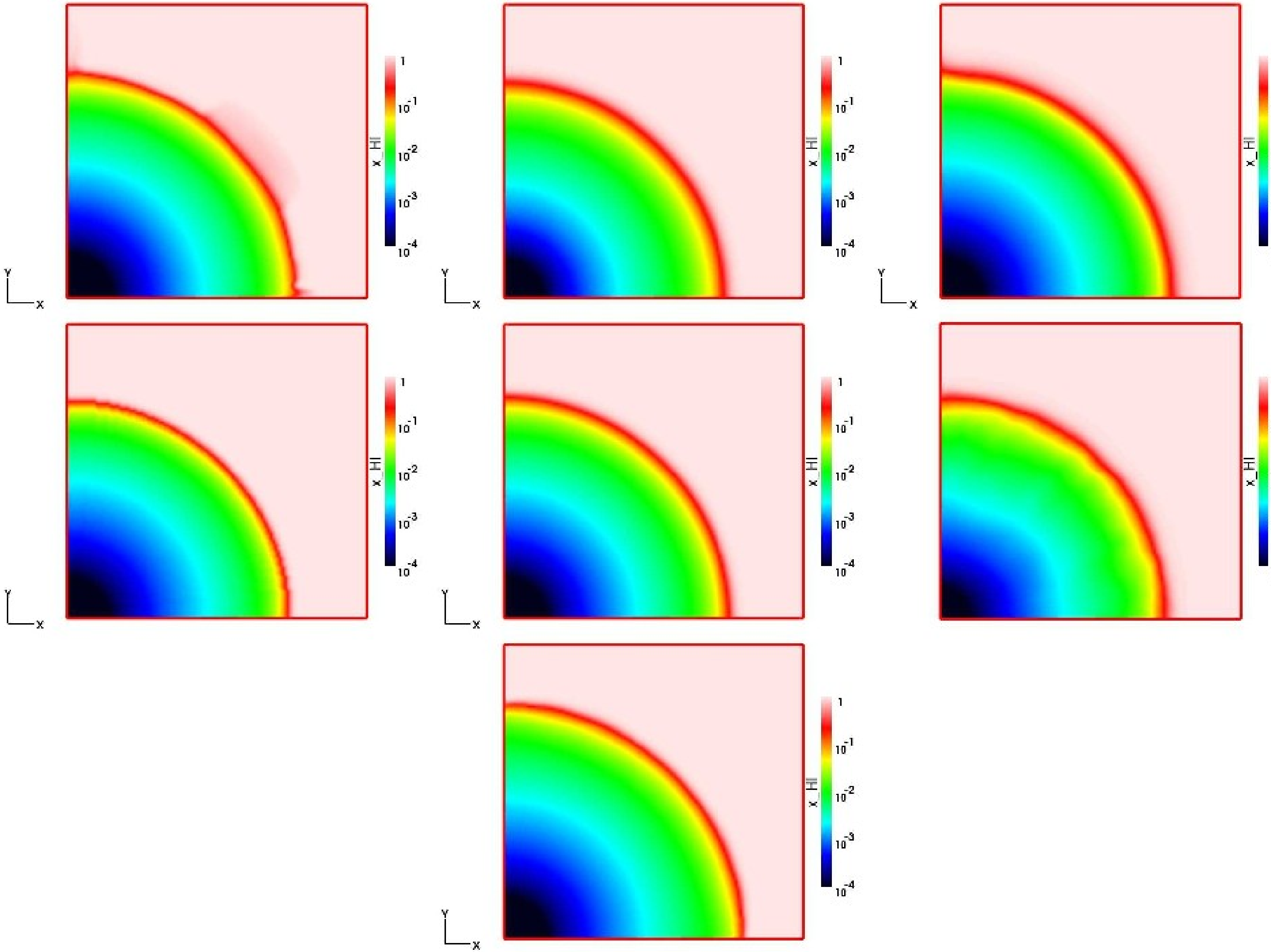

Figure 17. Test 6 (H II region gasdynamic expansion down a power-law initial density profile): Images of the H I fraction, cut through the simulation volume at coordinate $z = 0$ at time $t = 25$ Myr for (left to right) and top to bottom) C^2-Ray, HART, RSPH, ZEUS-MP, RH1D, LICORICE, and FLASH.

Test 6: the accelereting phase, temperature

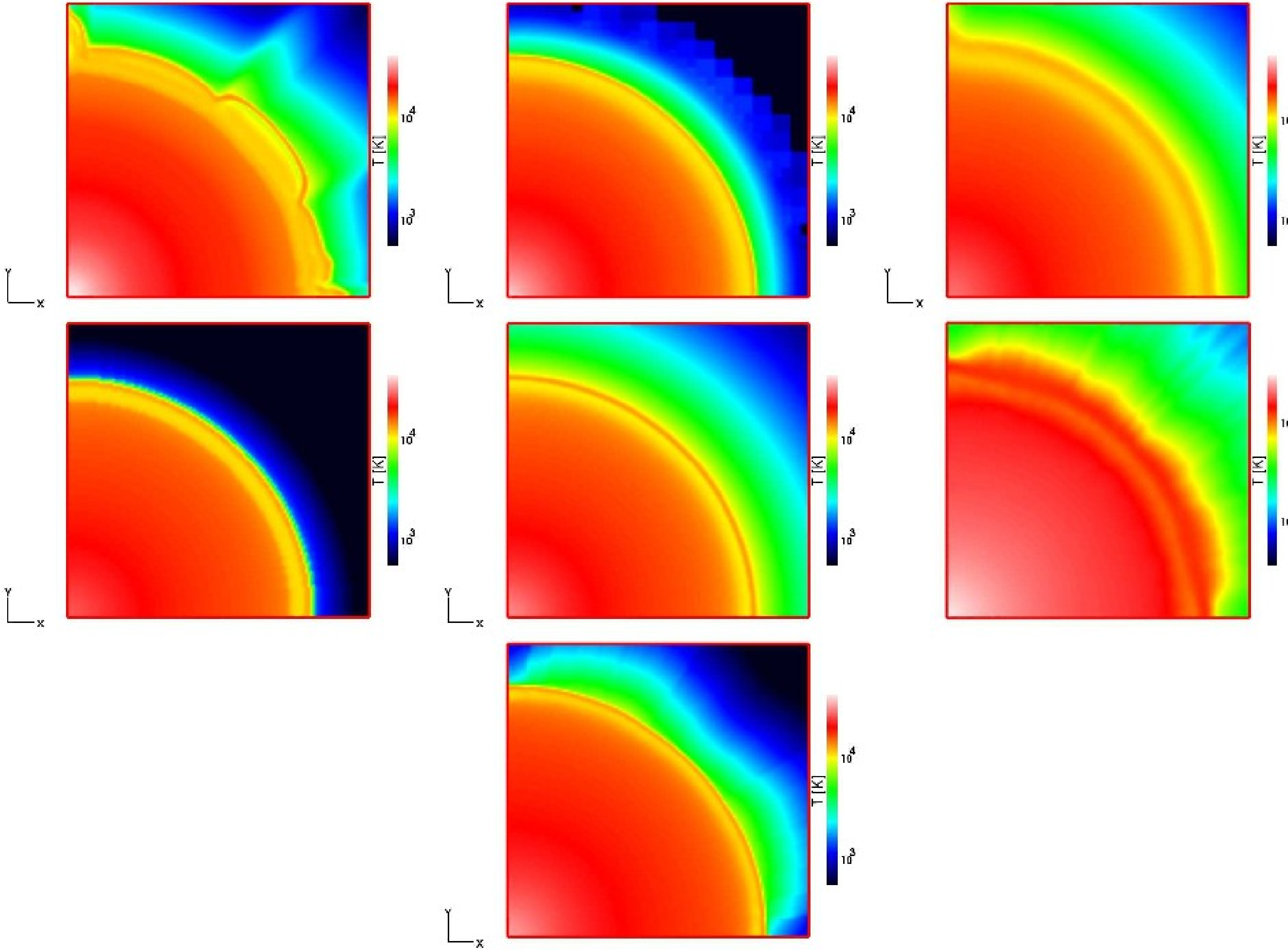

Figure 21. Test 6 (H II region gasdynamic expansion down a power-law initial density profile): Images of the temperature, cut through the simulation volume at coordinate $z = 0$ at time $t = 25$ Myr for (left to right) and top to bottom) C^2-Ray, HART, RSPH, ZEUS-MP, RH1D, LICORICE, and FLASH.

Test 6: the accelereting phase, HII

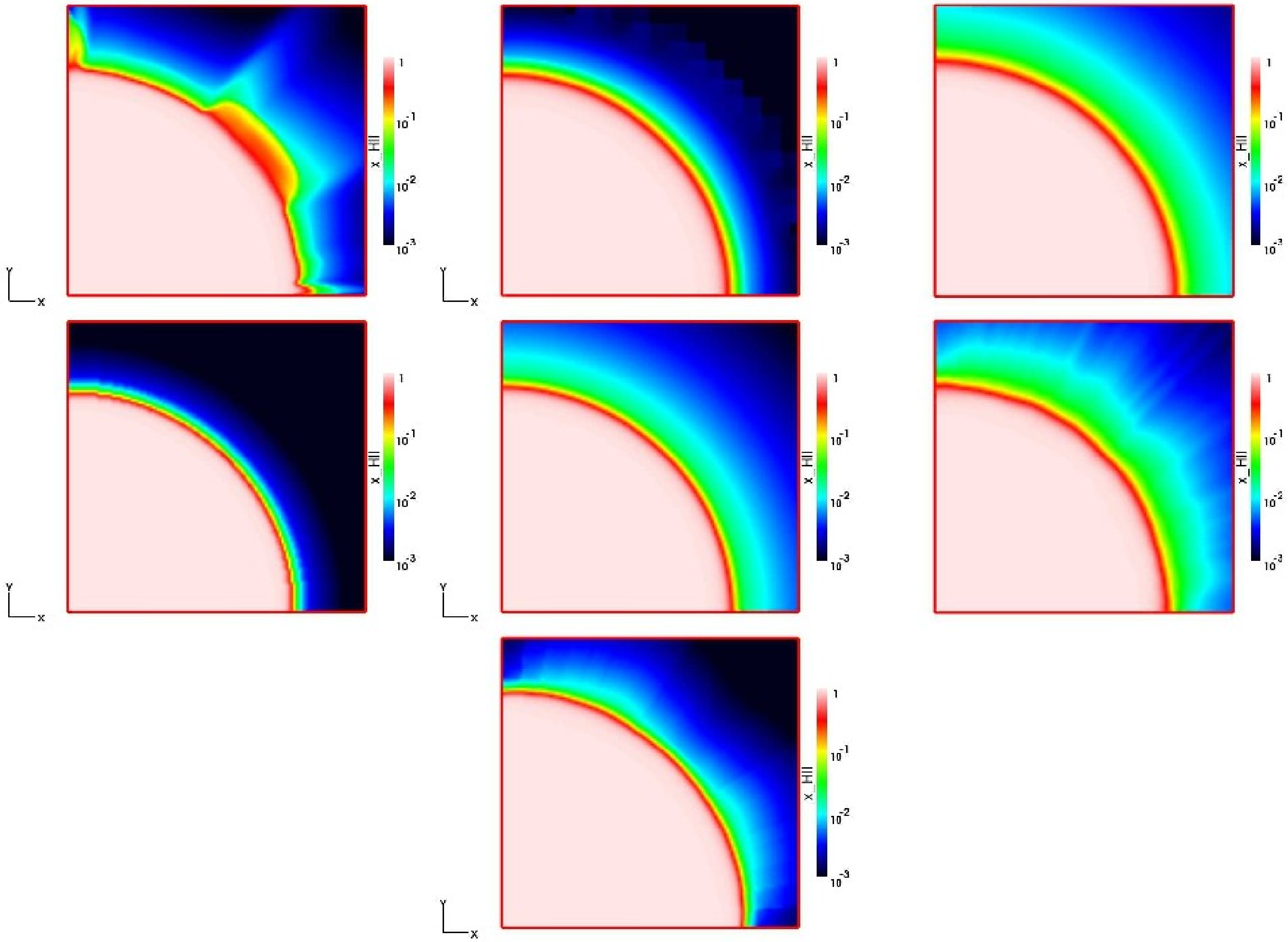

Figure 18. Test 6 (H II region gasdynamic expansion down a power-law initial density profile): Images of the H II fraction, cut through the simulation volume at coordinate $z = 0$ at time $t = 25$ Myr for (left to right) and top to bottom) C^2-Ray, HART, RSPH, ZEUS-MP, RH1D, LICORICE, and FLASH.

Test 6: the accelereting phase, density

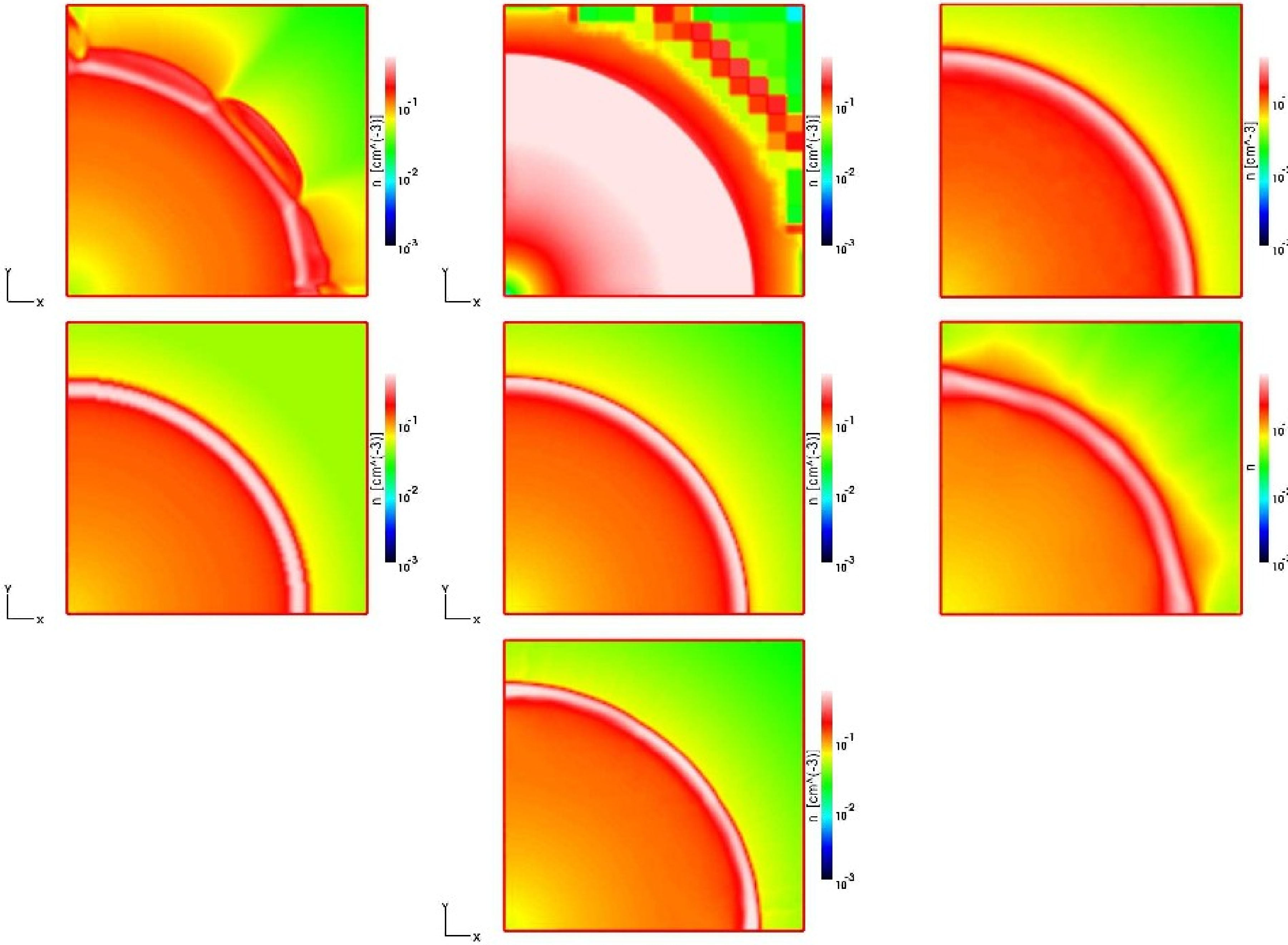

Figure 19. Test 6 (H II region gasdynamic expansion down a power-law initial density profile): Images of the density, cut through the simulation volume at coordinate $z = 0$ at time $t = 25$ Myr for (left to right) and top to bottom) C^2-Ray, HART, RSPH, ZEUS-MP, RH1D, LICORICE, and FLASH.

Test 6: the accelereting phase, Mach

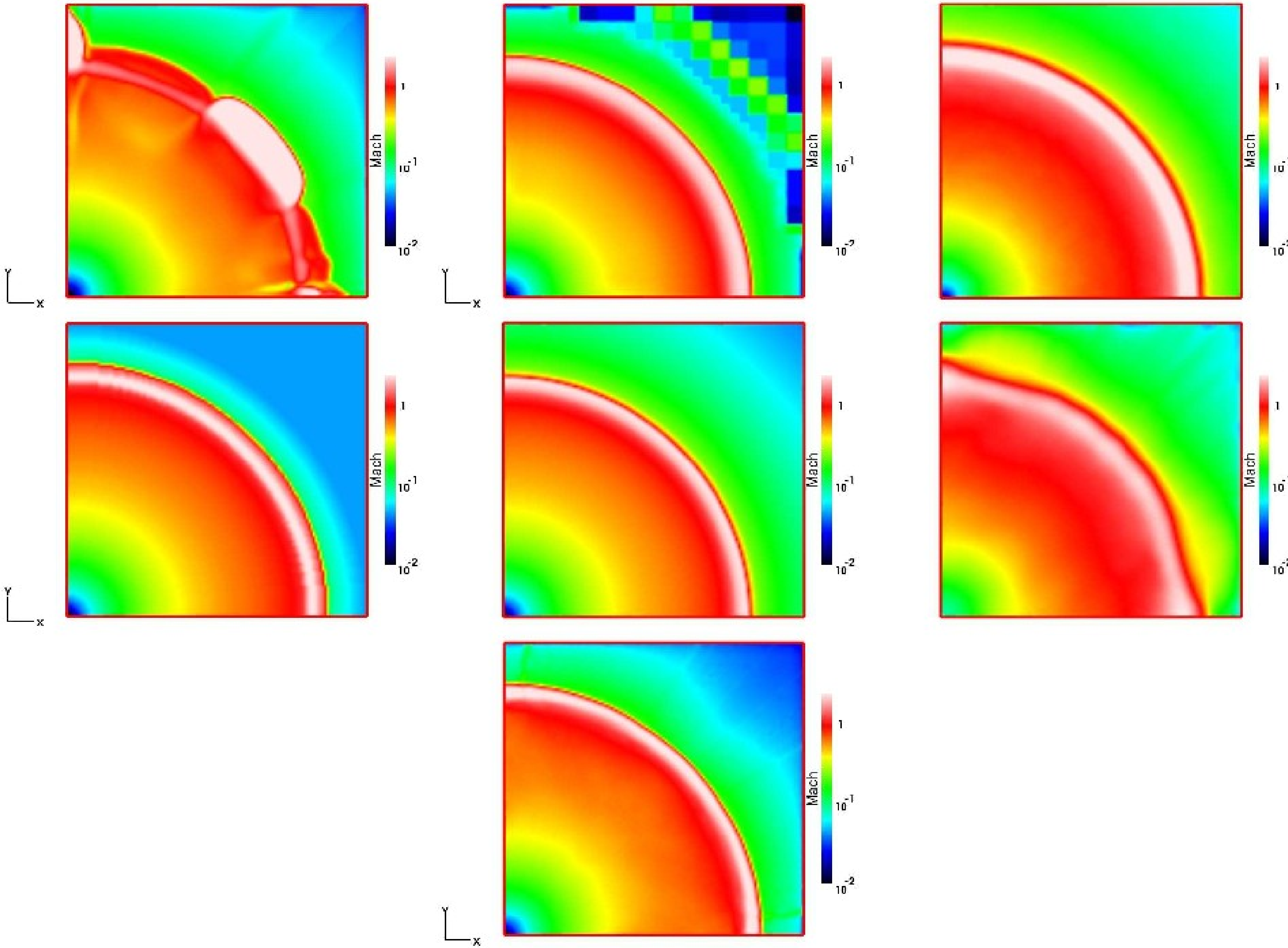

Figure 20. Test 6 (H II region gasdynamic expansion down a power-law initial density profile): Images of the Mach number, cut through the simulation volume at coordinate $z = 0$ at time $t = 25$ Myr for (left to right) and top to bottom) C^2-Ray, HART, RSPH, ZEUS-MP, RH1D, LICORICE, and FLASH.

Test 6: I-front position and velocity

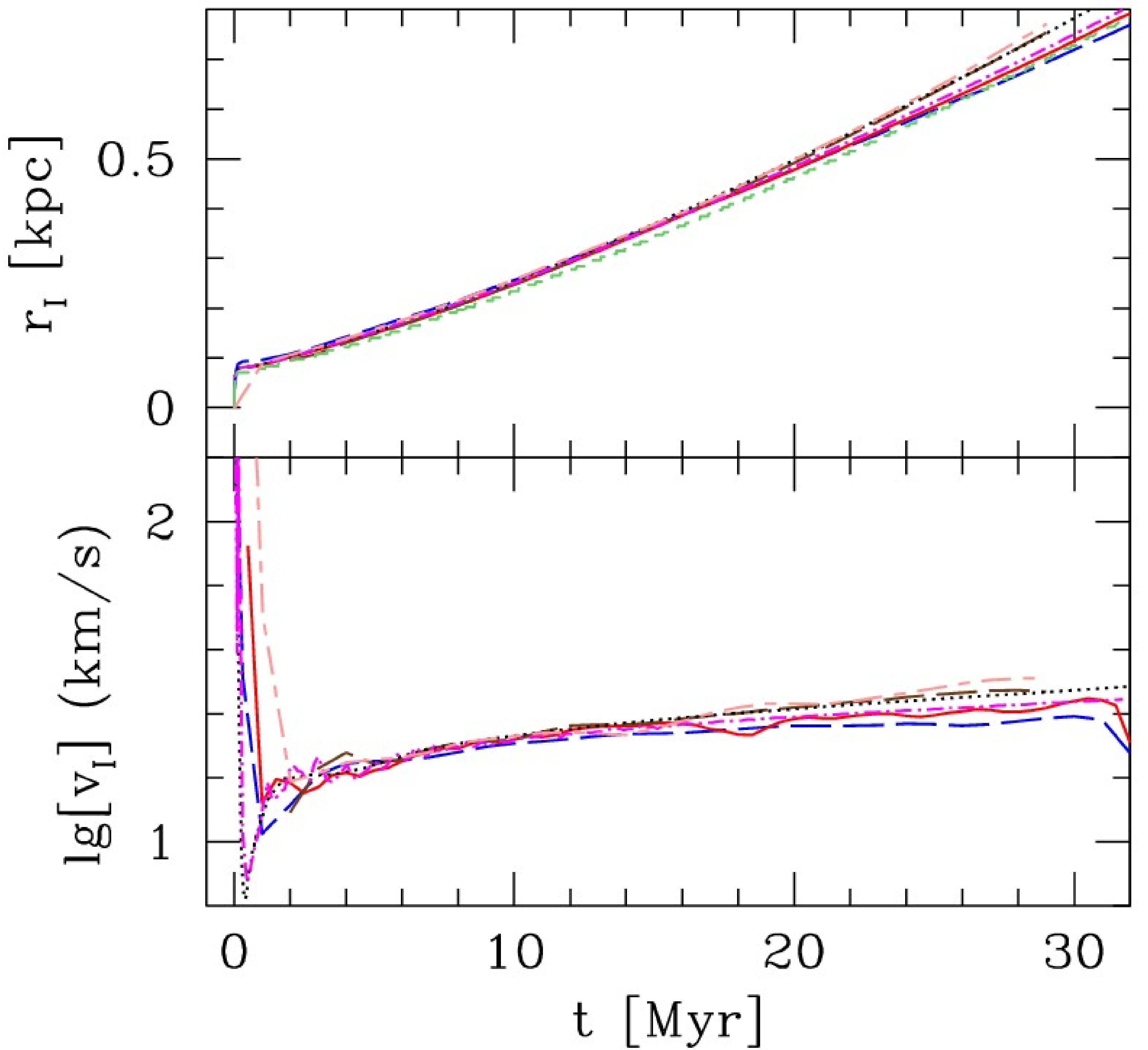

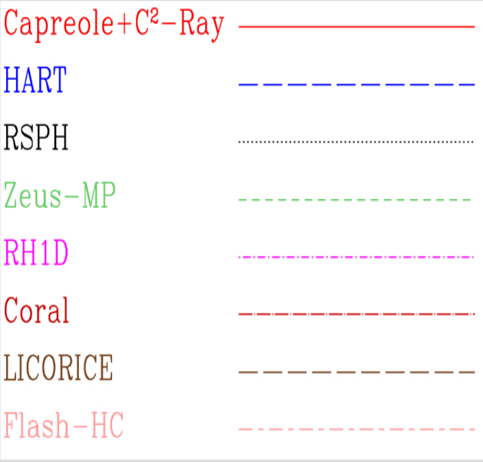

Test 6: Ionization & density structure

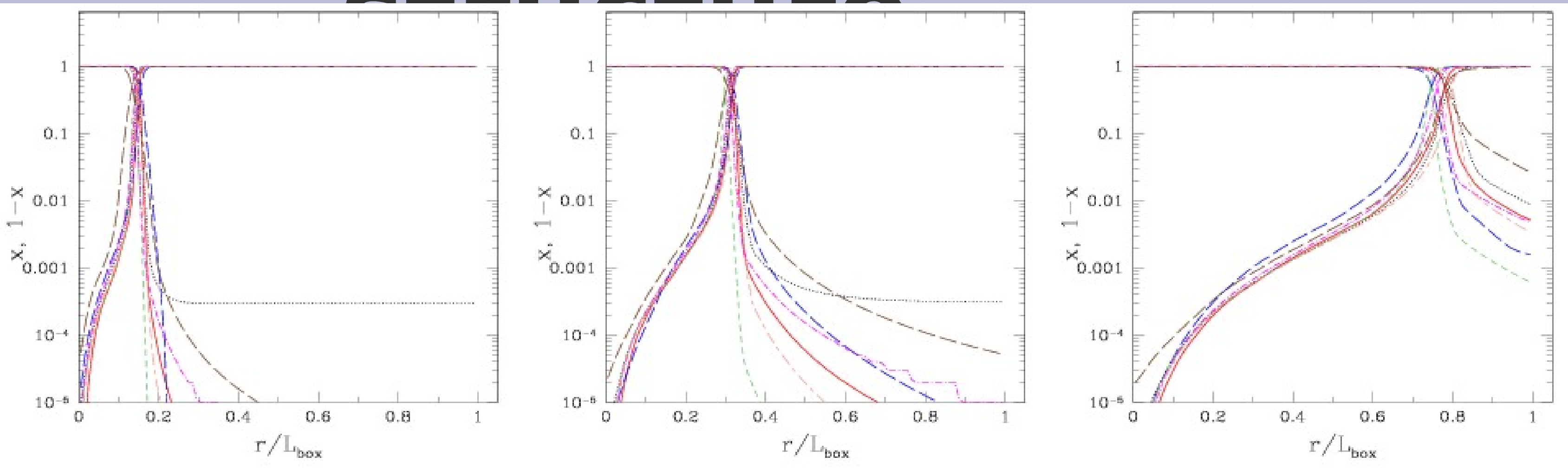

Figure 23. Test 6 (H II region gasdynamic expansion down a power-law initial density profile): Spherically-averaged profiles for ionized fractions x and neutral fractions $x_{\rm HI} = 1 - x$ at times $t = 3$ Myr, 10 Myr and 25 Myr vs. dimensionless radius (in units of the box size).

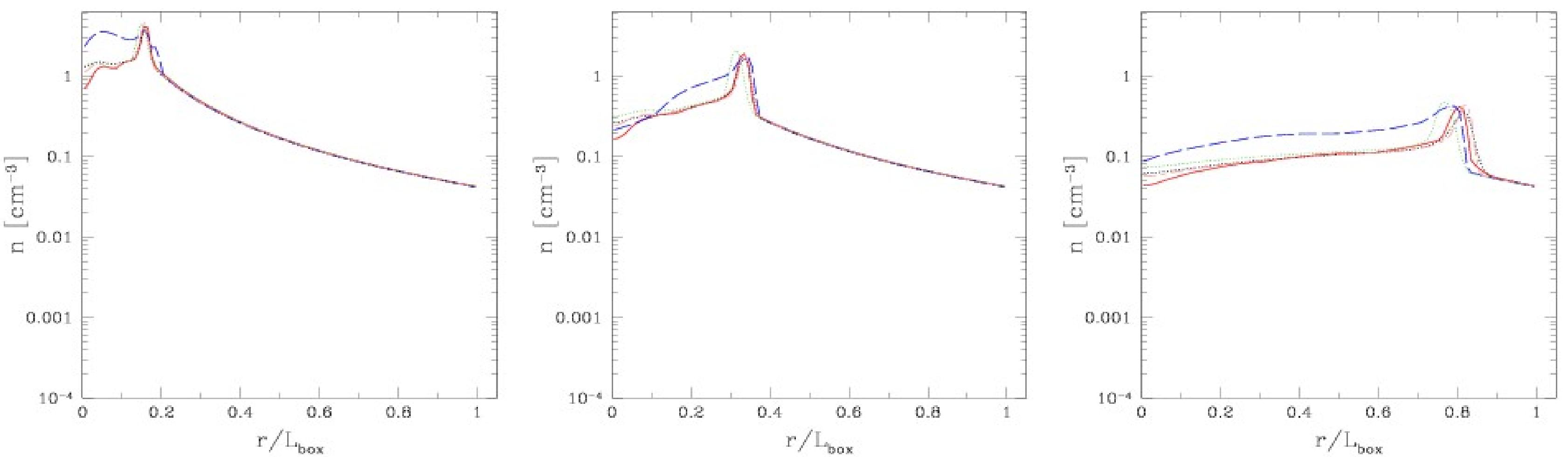

Figure 24. Test 6 (H II region gasdynamic expansion down a power-law initial density profile): Spherically-averaged profiles for the gas number density, n, at times $t = 3$ Myr, 10 Myr and 25 Myr vs. dimensionless radius (in units of the box size).

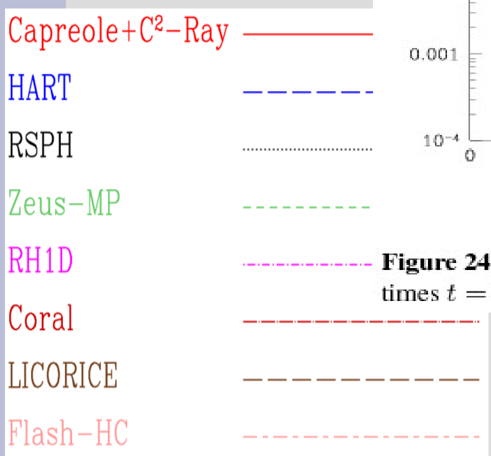

Test 6: temp. and Mach structure

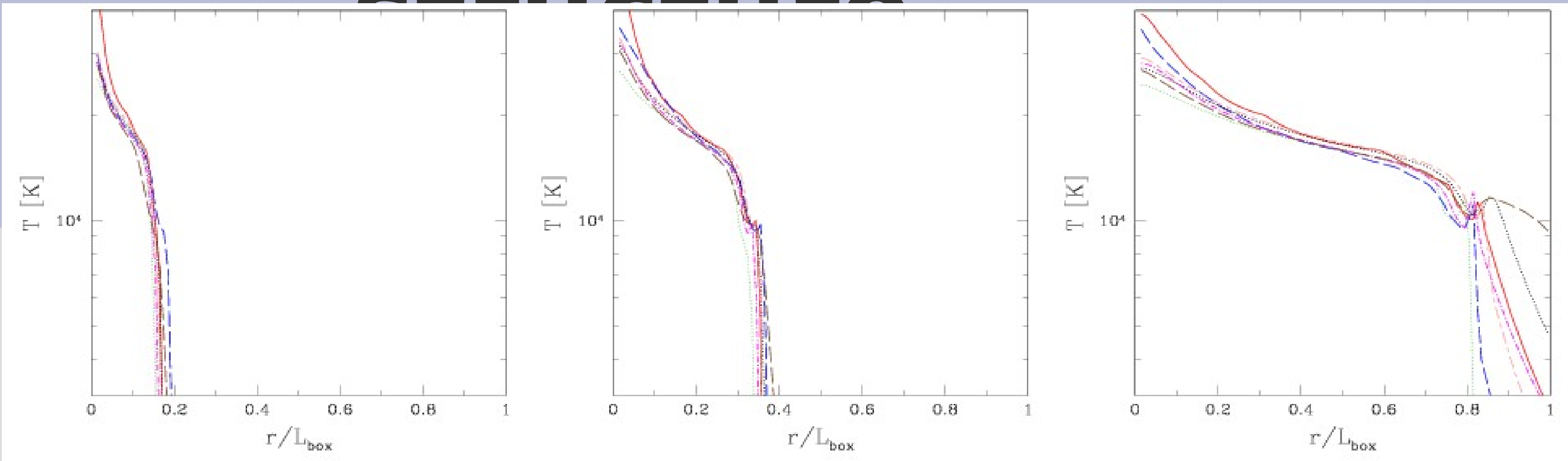

Figure 26. Test 6 (H II region gasdynamic expansion down a power-law initial density profile): Spherically-averaged profiles for temperature at times t = 3 Myr, 10 Myr and 25 Myr vs. dimensionless radius (in units of the box size).

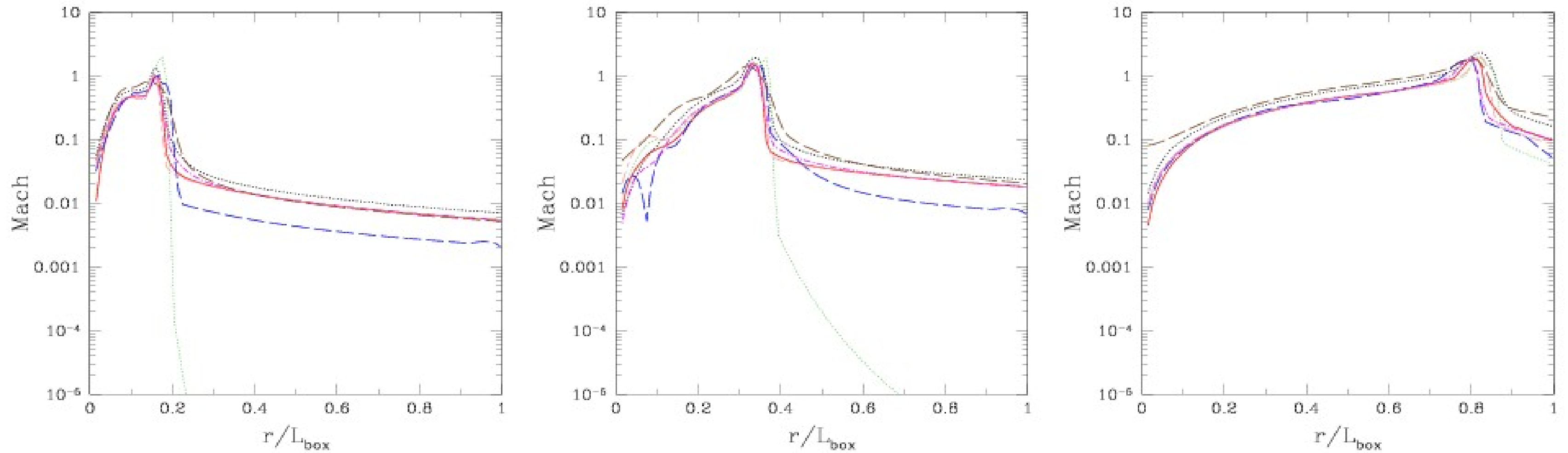

Figure 27. Test 6 (H II region gasdynamic expansion down a power-law initial density profile): Spherically-averaged profiles of the Mach number at times t = 3 Myr, 10 Myr and 25 Myr vs. dimensionless radius (in units of the box size).

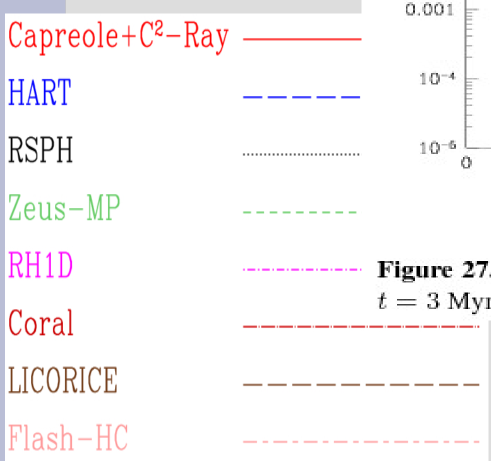

Test 6: pressure structure

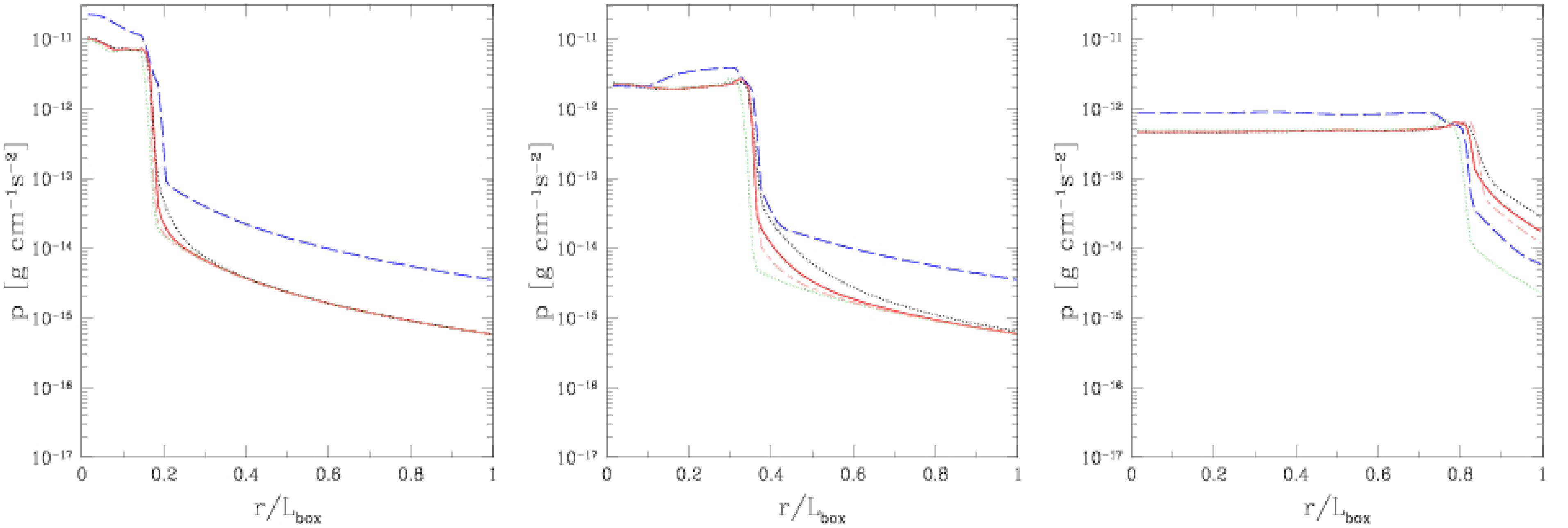

Figure 25. Test 6 (H II region gasdynamic expansion down a power-law initial density profile): Spherically-averaged profiles for pressure, p, at times t = 3 Myr, 10 Myr and 25 Myr vs. dimensionless radius (in units of the box size).

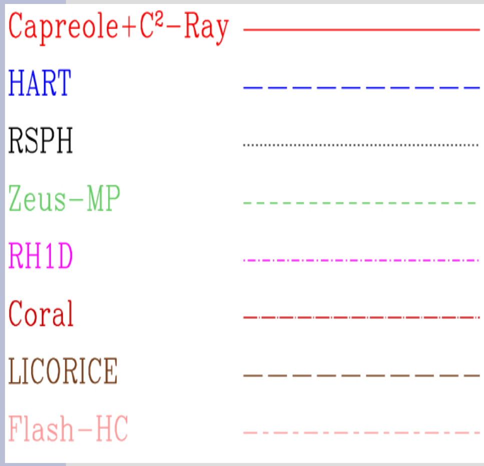

Test 7: initial trapping phase, ion. structure

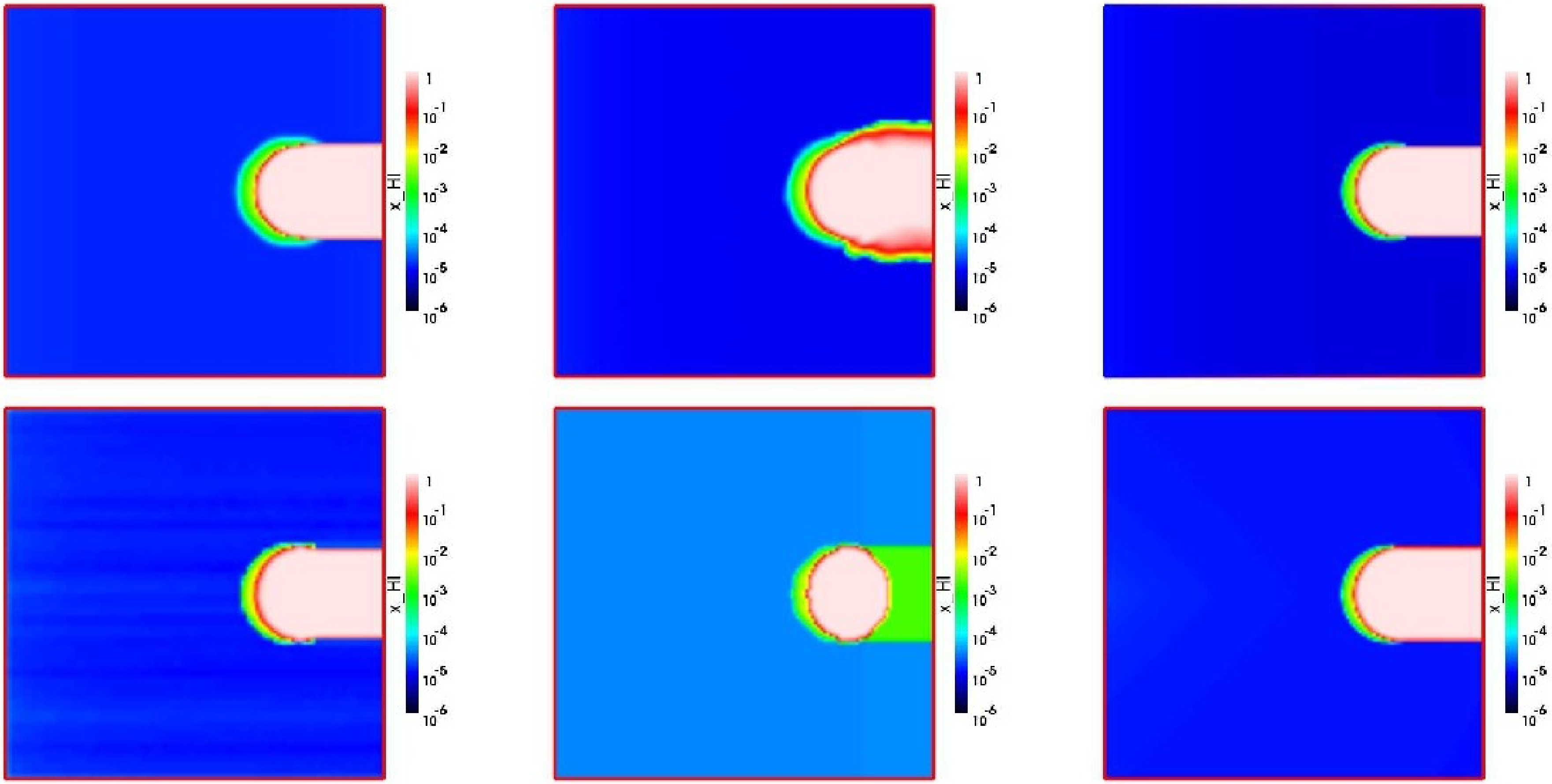

Figure 28. Test 7 (Photoevaporation of a dense clump.): Images of the H I fraction, cut through the simulation volume at coordinate $z = 0$ at time $t = 1$ Myr for (left to right and top to bottom) C^2-Ray, RSPH, ZEUS-MP, and LICORICE, FLASH and Coral.

Test 7: early photoevaporation phase, ion. structure

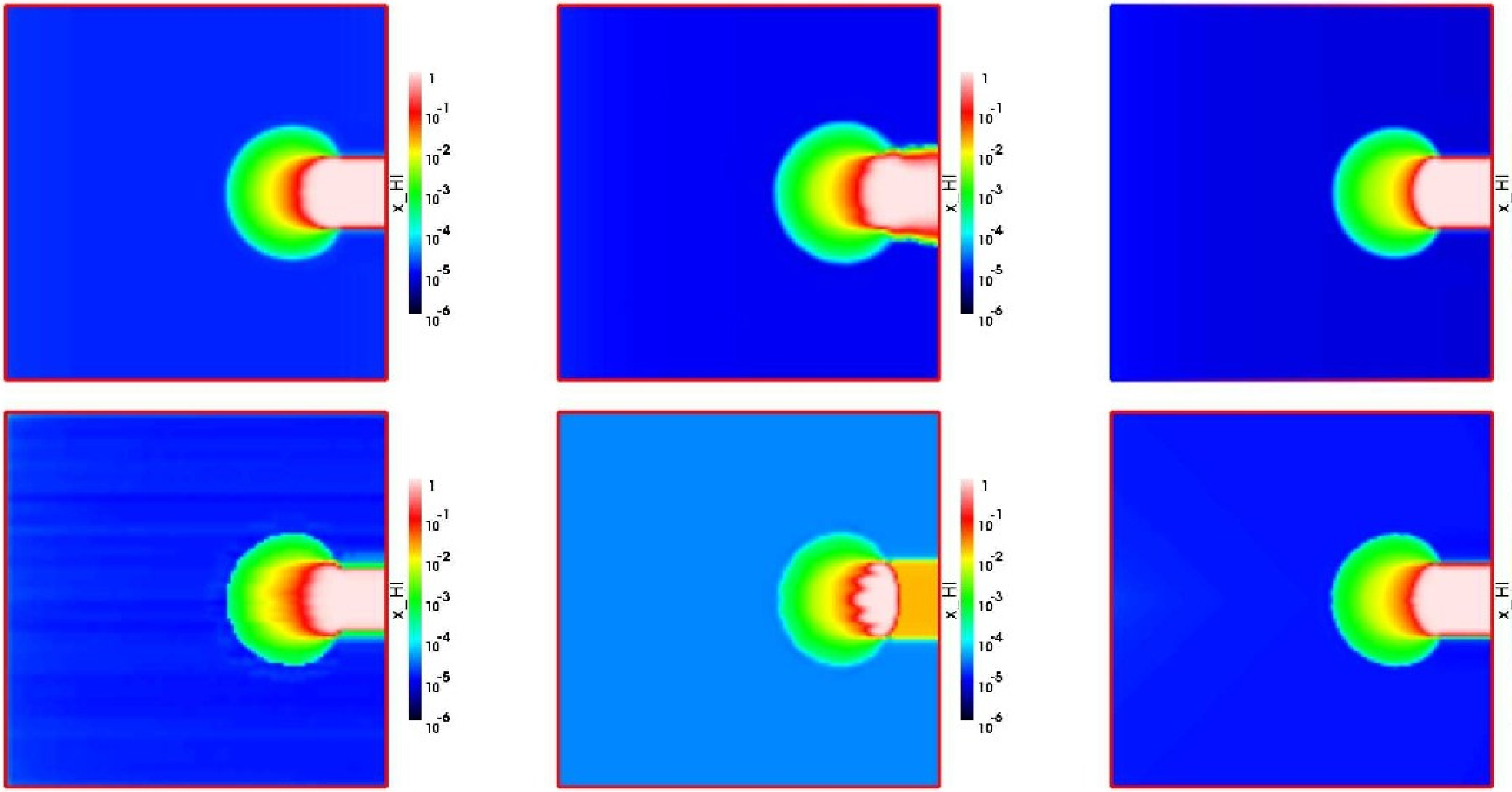

Figure 29. Test 7 (Photoevaporation of a dense clump.): Images of the H I fraction, cut through the simulation volume at coordinate $z = 0$ at time $t = 10$ Myr for (left to right and top to bottom) C^2-Ray, RSPH, ZEUS-MP, and LICORICE, FLASH and Coral.

Test 7: early photoevaporation phase, temperature

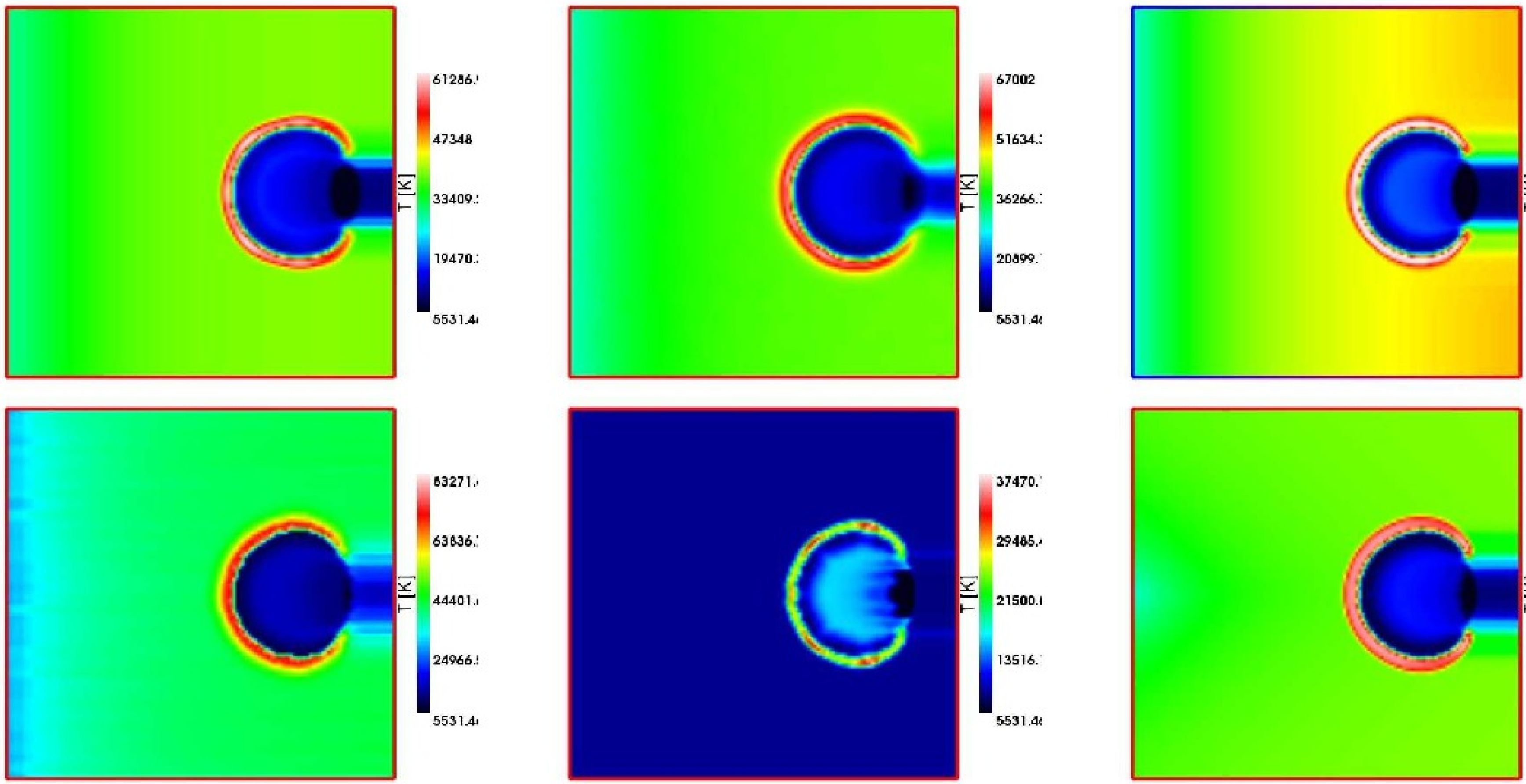

ure 31. Test 7 (Photoevaporation of a dense clump.): Images of the gas temperature, cut through the simulation volume at coordinate $z = 0$ at time $t = 10$
for (left to right and top to bottom) C^2-Ray, RSPH, ZEUS-MP, and LICORICE, FLASH and Coral.

Test 7: early photoevaporation phase, pressure

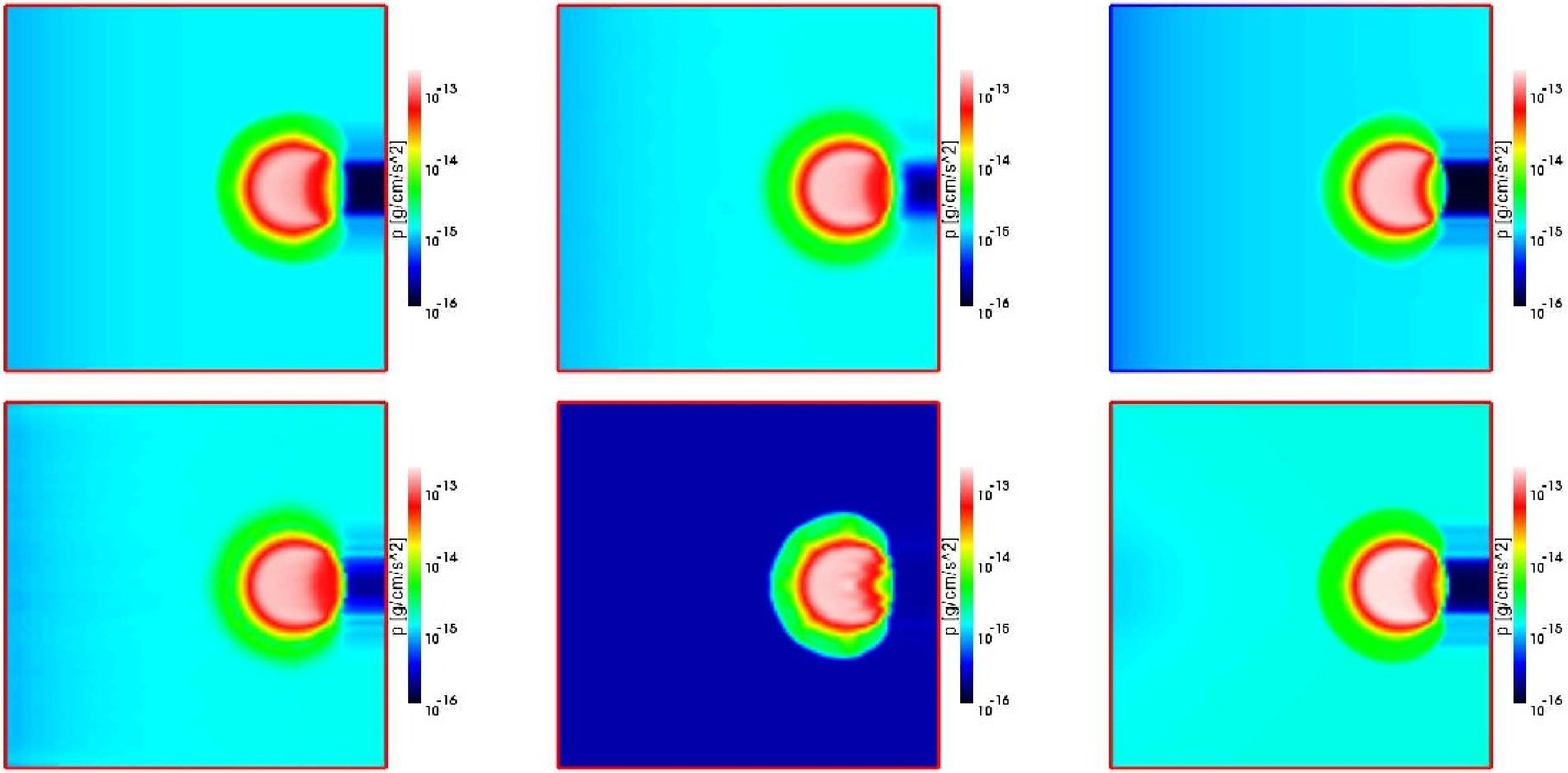

ure 30. Test 7 (Photoevaporation of a dense clump.): Images of the gas pressure, cut through the simulation volume at coordinate $z = 0$ at time $t = 10$ for (left to right and top to bottom) C^2-Ray, RSPH, ZEUS-MP, and LICORICE, FLASH and Coral.

Test 7: early photoevaporation phase, Mach number

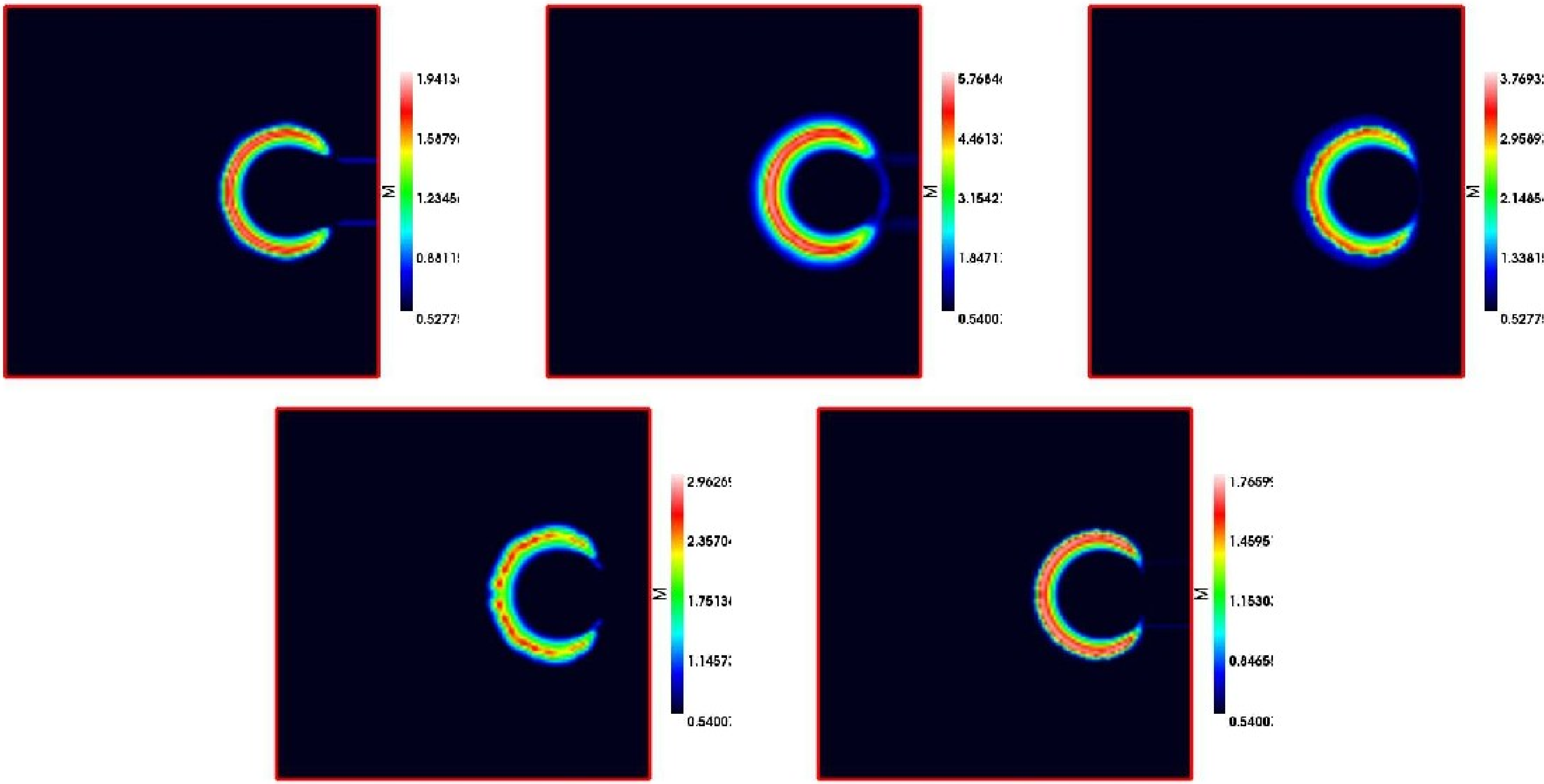

Figure 32. Test 7 (Photoevaporation of a dense clump.): Images of the flow Mach number, cut through the simulation volume at coordinate $z = 0$ at time $t = 10$ Myr for (left to right and top to bottom) C^2-Ray, RSPH, and LICORICE, FLASH and Coral.

Test 7: late photoevaporation phase: ion. structure

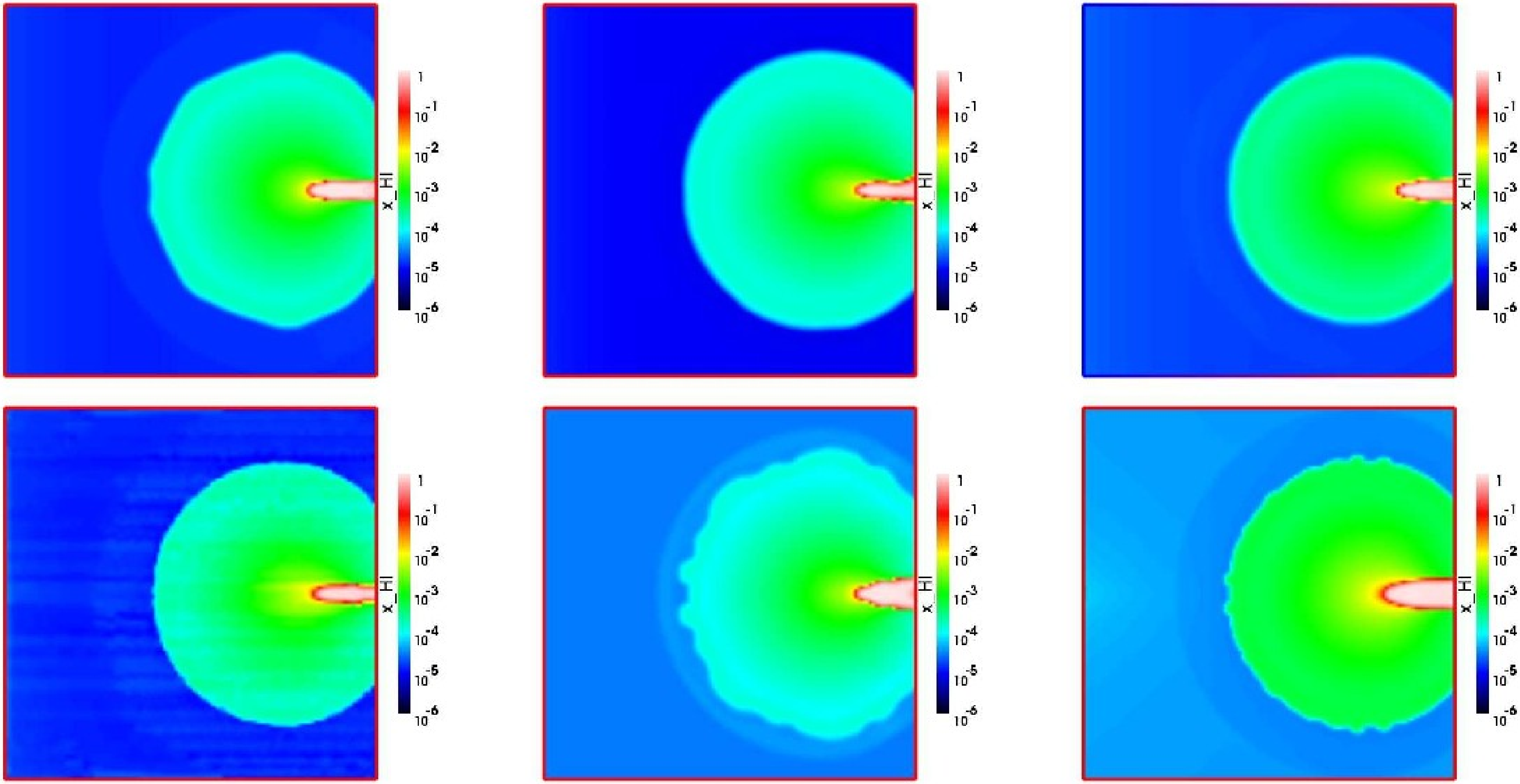

Figure 33. Test 7 (Photoevaporation of a dense clump.): Images of the H I fraction, cut through the simulation volume at coordinate $z = 0$ at time $t = 50$ Myr for (left to right and top to bottom) C^2-Ray, RSPH, ZEUS-MP, and LICORICE, FLASH and Coral.

Test 7: late photoevaporation phase: temperature

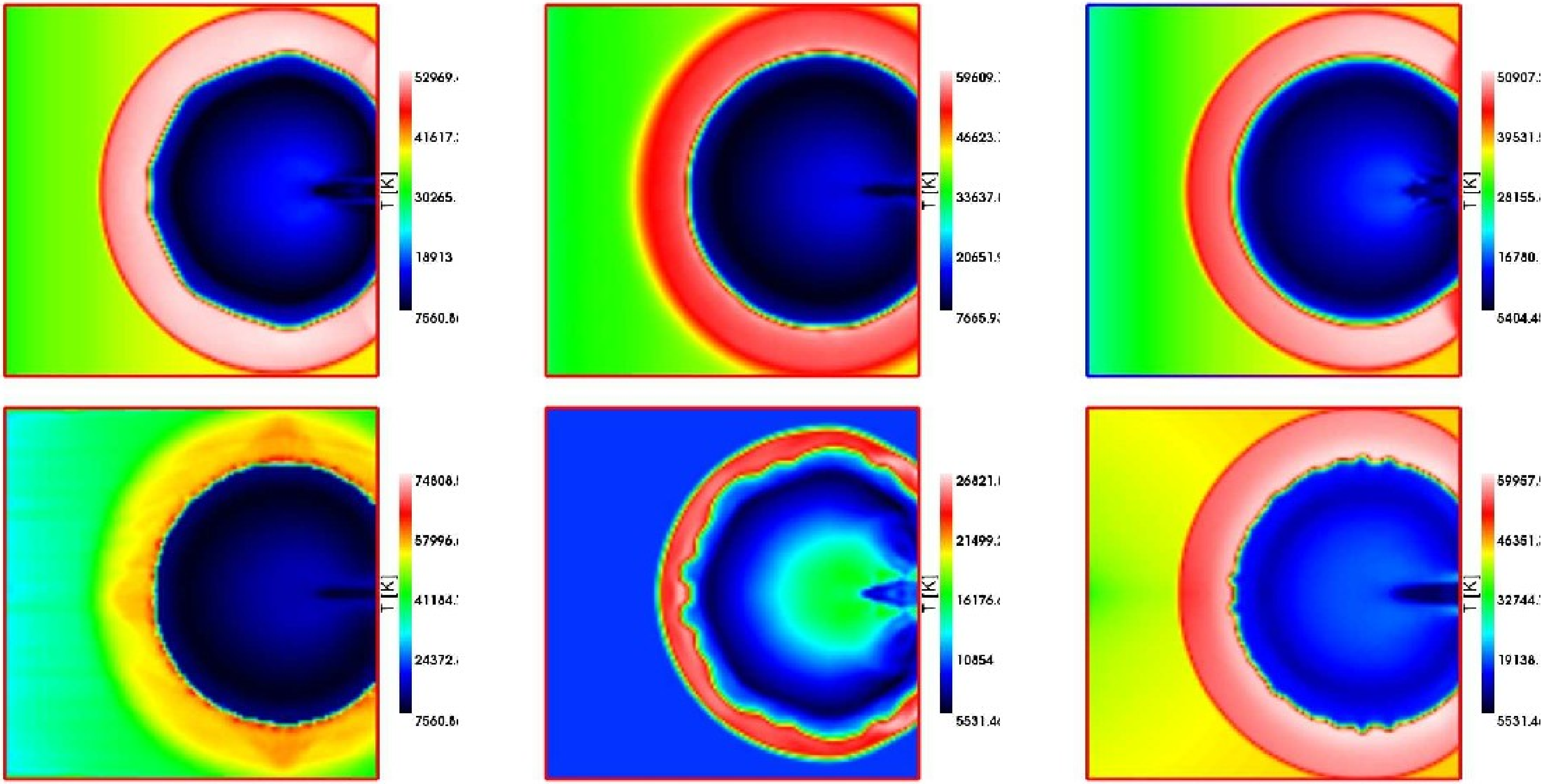

Figure 35. Test 7 (Photoevaporation of a dense clump.): Images of the temperature, cut through the simulation volume at coordinate $z = 0$ at time $t = 50$ Myr for (left to right and top to bottom) C^2-Ray, RSPH, ZEUS-MP, and LICORICE, FLASH and Coral.

Test 7: late photoevaporation phase: pressure

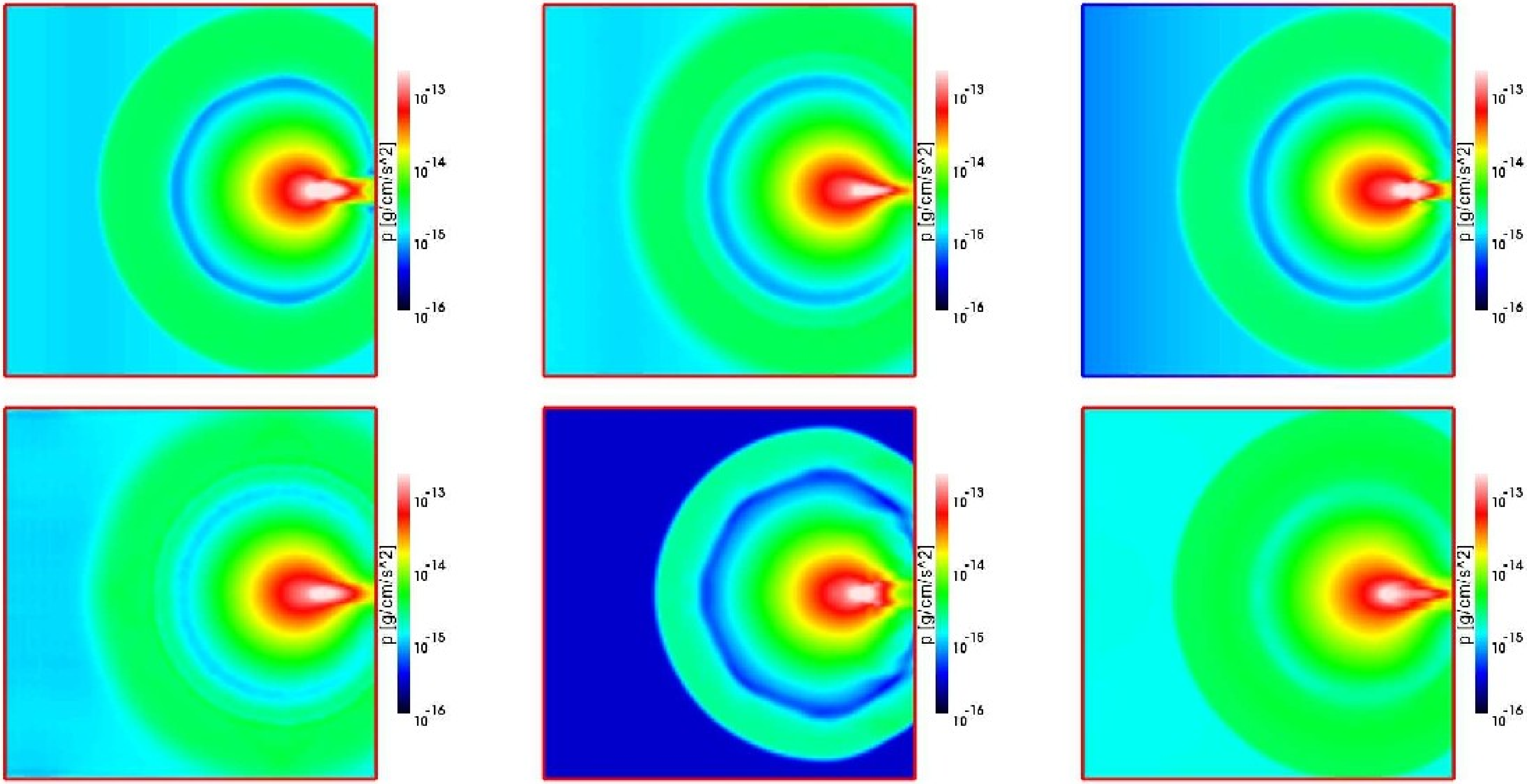

Figure 34. Test 7 (Photoevaporation of a dense clump.): Images of the pressure, cut through the simulation volume at coordinate $z = 0$ at time $t = 50$ Myr for (left to right and top to bottom) C^2-Ray, RSPH, ZEUS-MP, and LICORICE, FLASH and Coral.

Test 7: late photoevaporation phase: Mach number

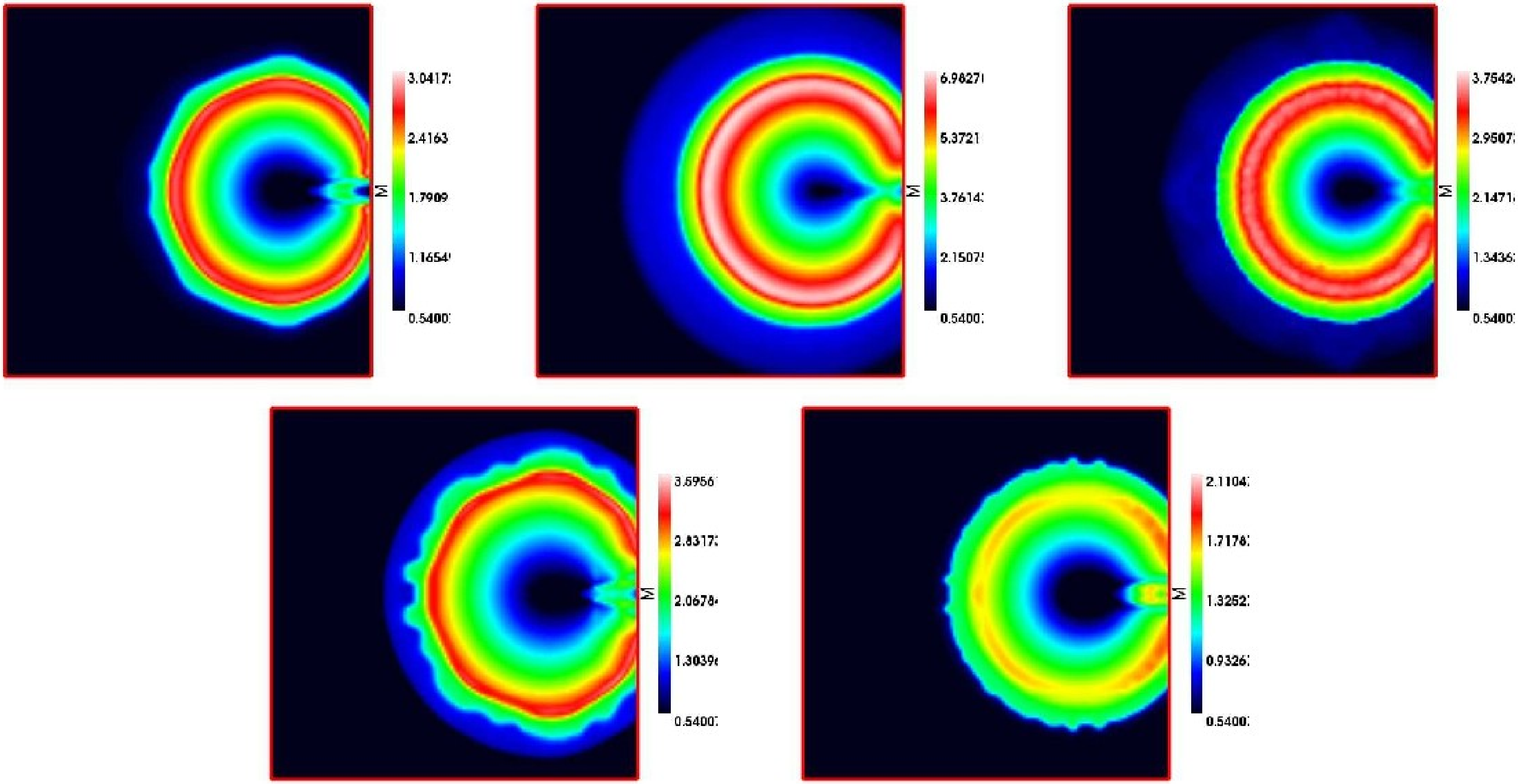

Figure 36. Test 7 (Photoevaporation of a dense clump): Images of the flow Mach number, cut through the simulation volume at coordinate $z = 0$ at time $t = 50$ Myr for (left to right and top to bottom) C^2-Ray, RSPH, and LICORICE, FLASH and Coral.

Test 7: I-front position and velocity

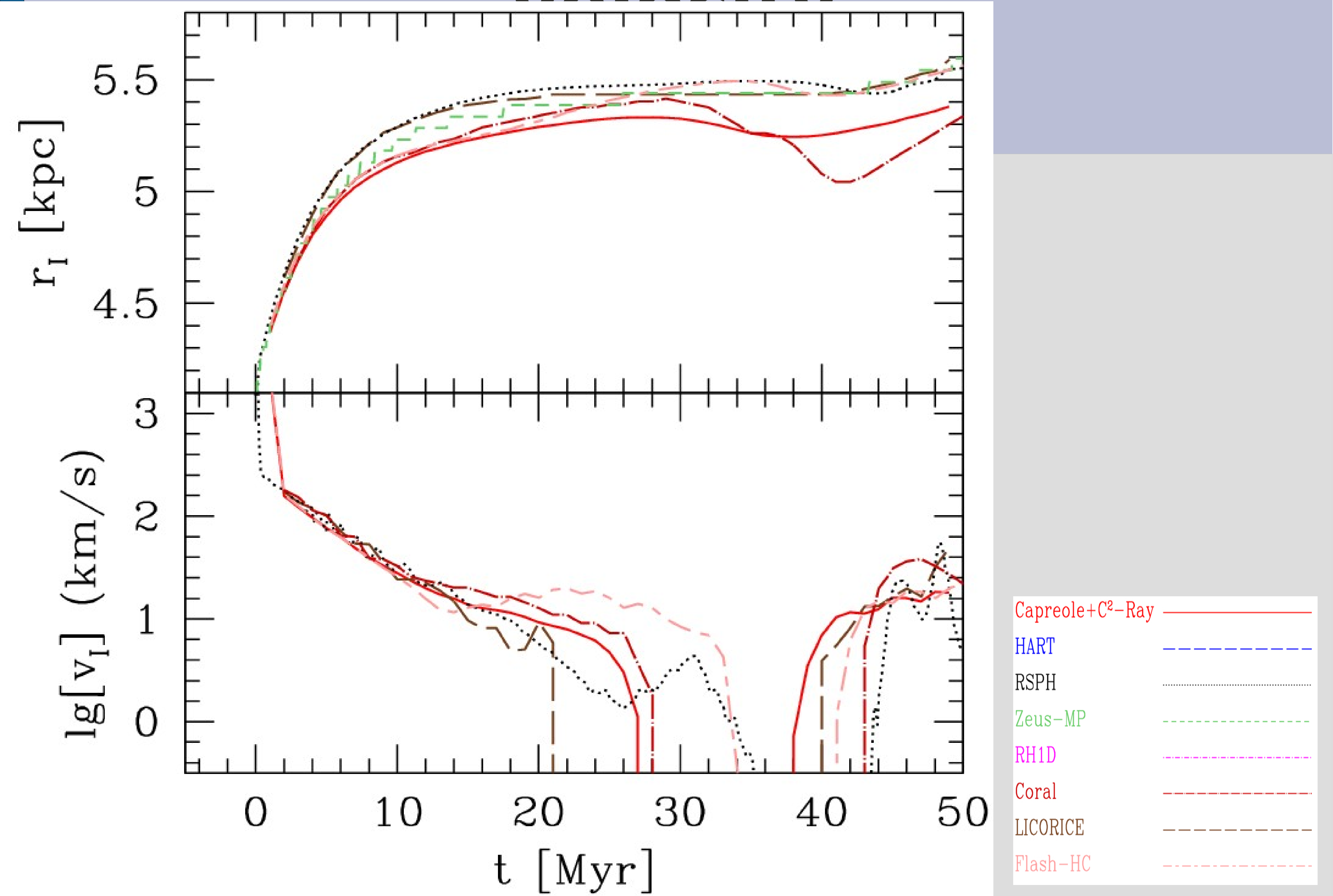

Test 7: Ionization & temperature cuts

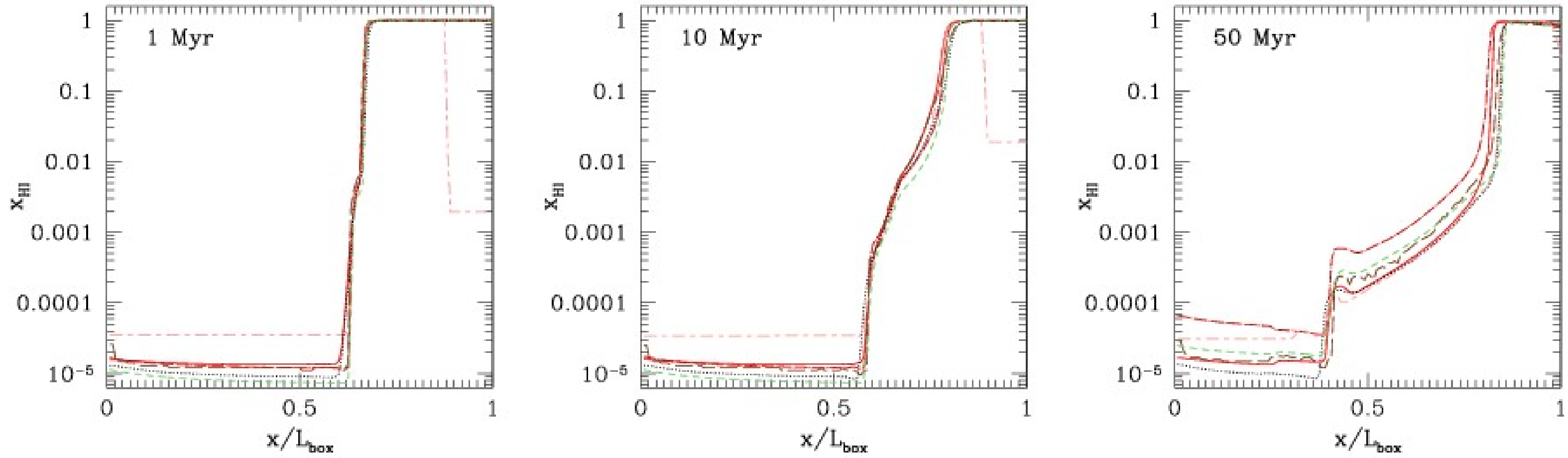

Figure 40. Test 7 (Photoevaporation of a dense clump): Line cuts of the neutral fraction along the axis of symmetry through the centre of the clump at times $t = 1$ Myr, 10 Myr and 50 Myr (left to right).

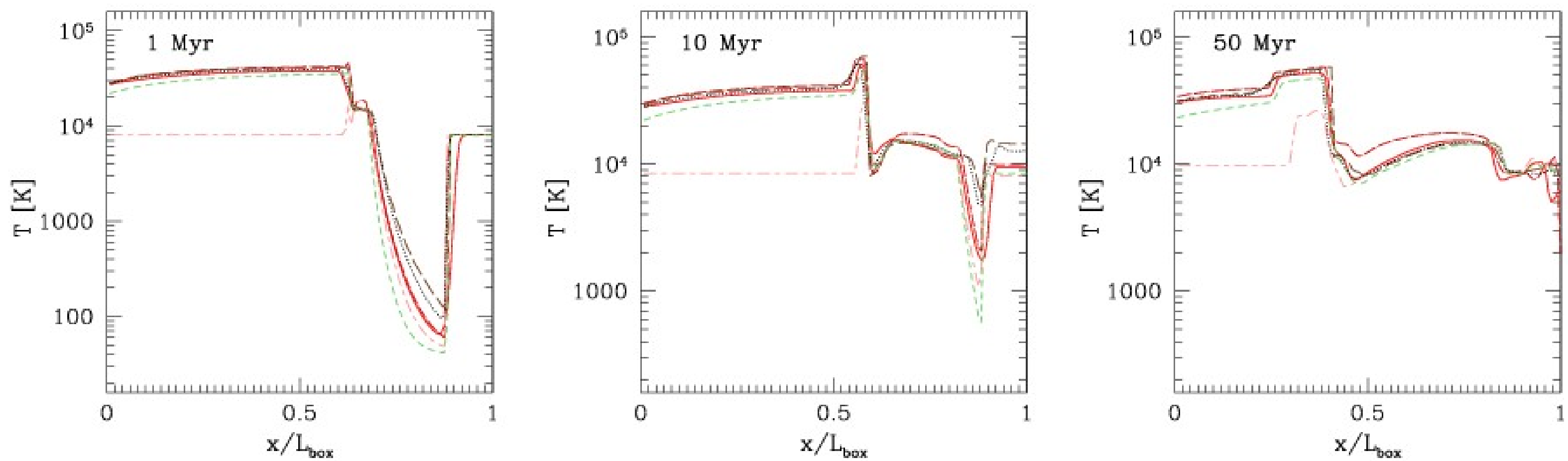

Figure 41. Test 7 (Photoevaporation of a dense clump): Line cuts of the temperature along the axis of symmetry through the centre of the clump at times $t = 1$ Myr, 10 Myr and 50 Myr (left to right).

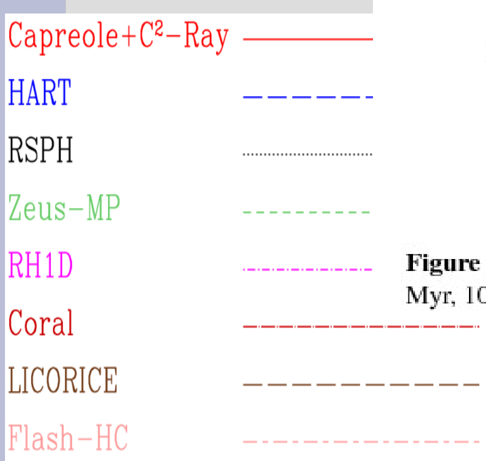

Test 7: ionization & temperature cuts

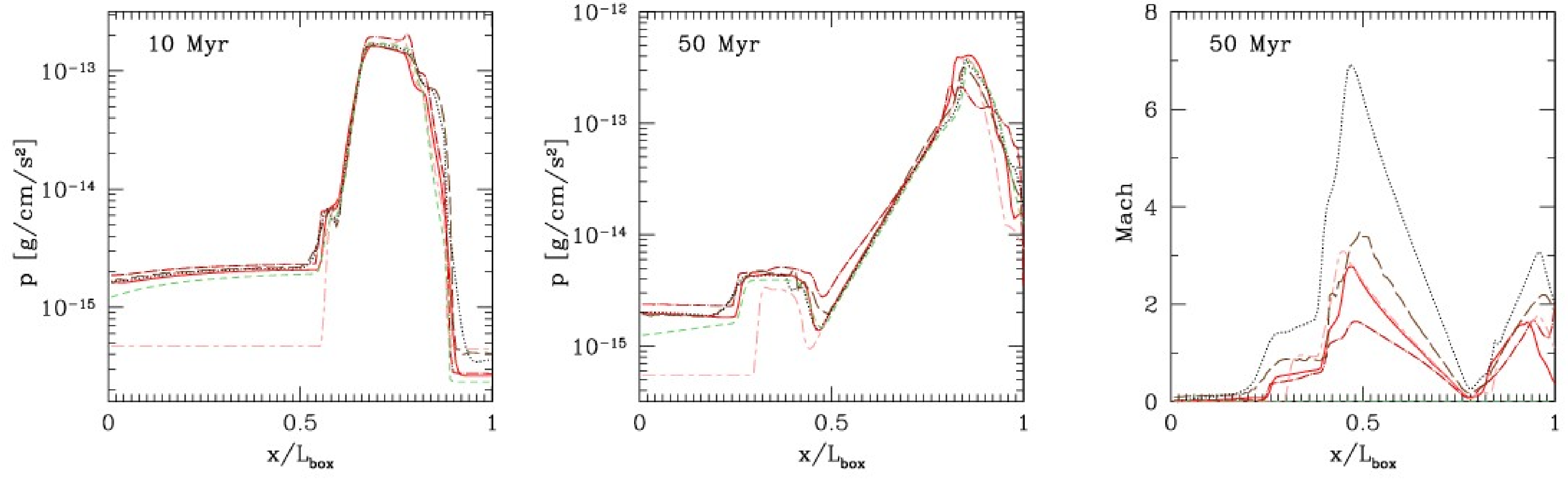

Figure 42. Test 7 (Photoevaporation of a dense clump): Line cuts of the pressure at times $t = 10$ Myr (left), and 50 Myr (centre) and of the Mach number at time $t = 50$ Myr (right) along the axis of symmetry through the centre of the clump.

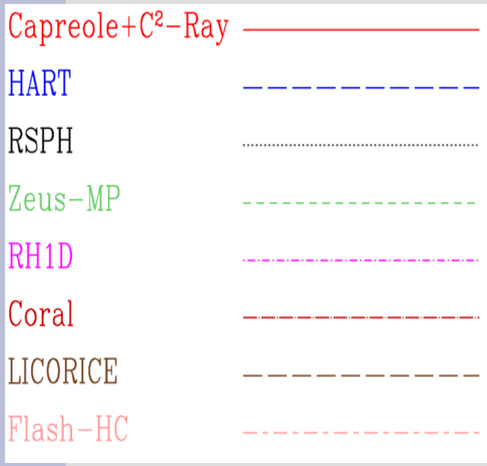

Test 7: Ionization & temp. histograms

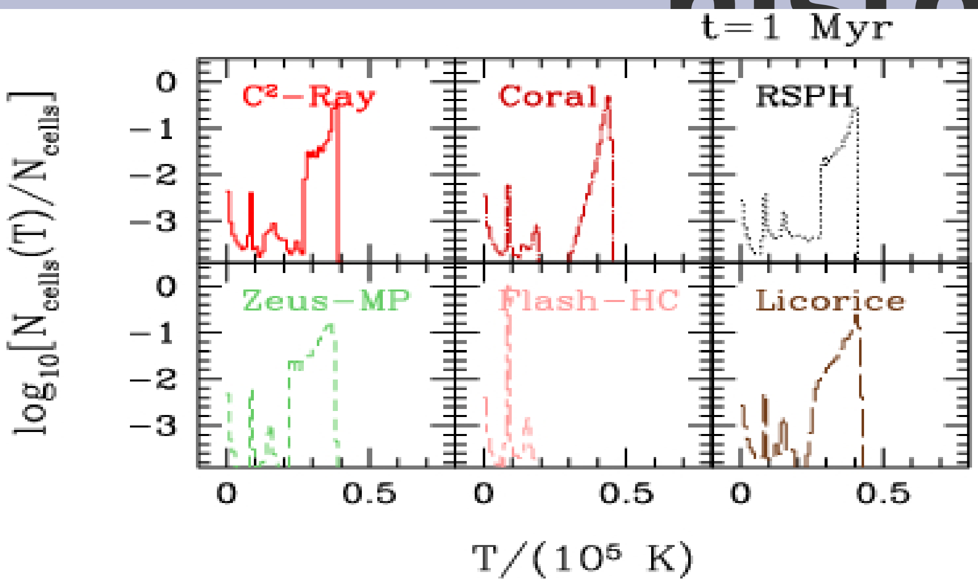

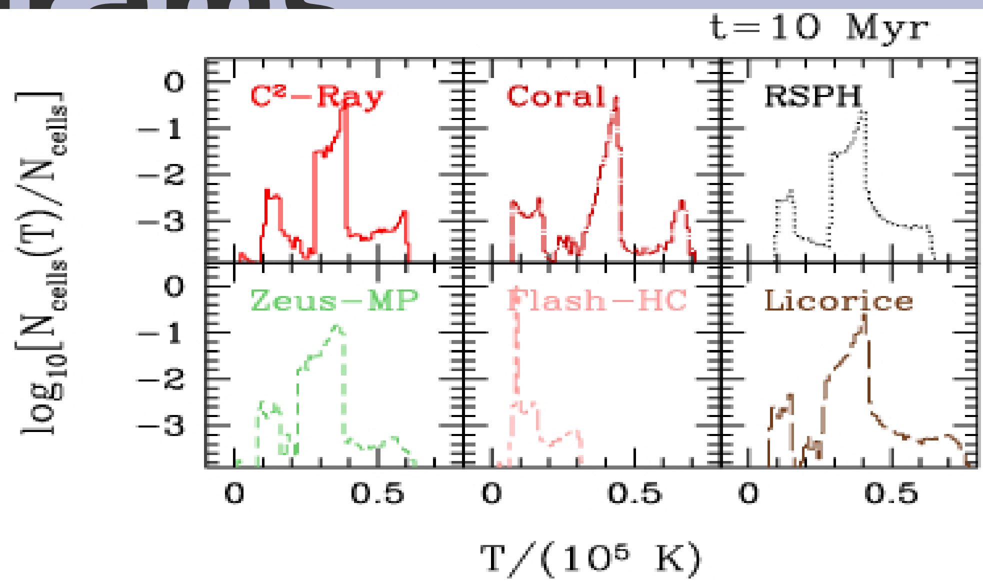

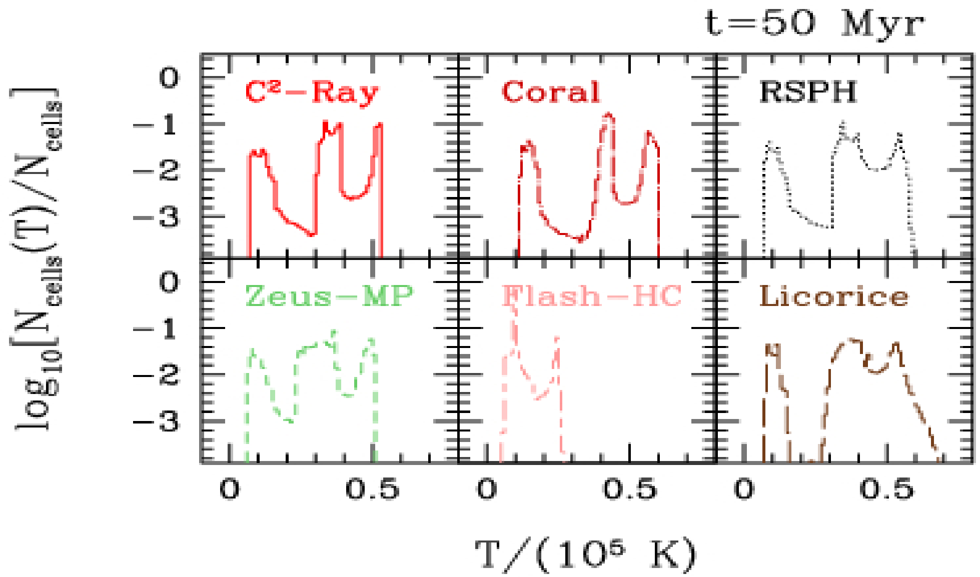

Test 7: Mach number histograms

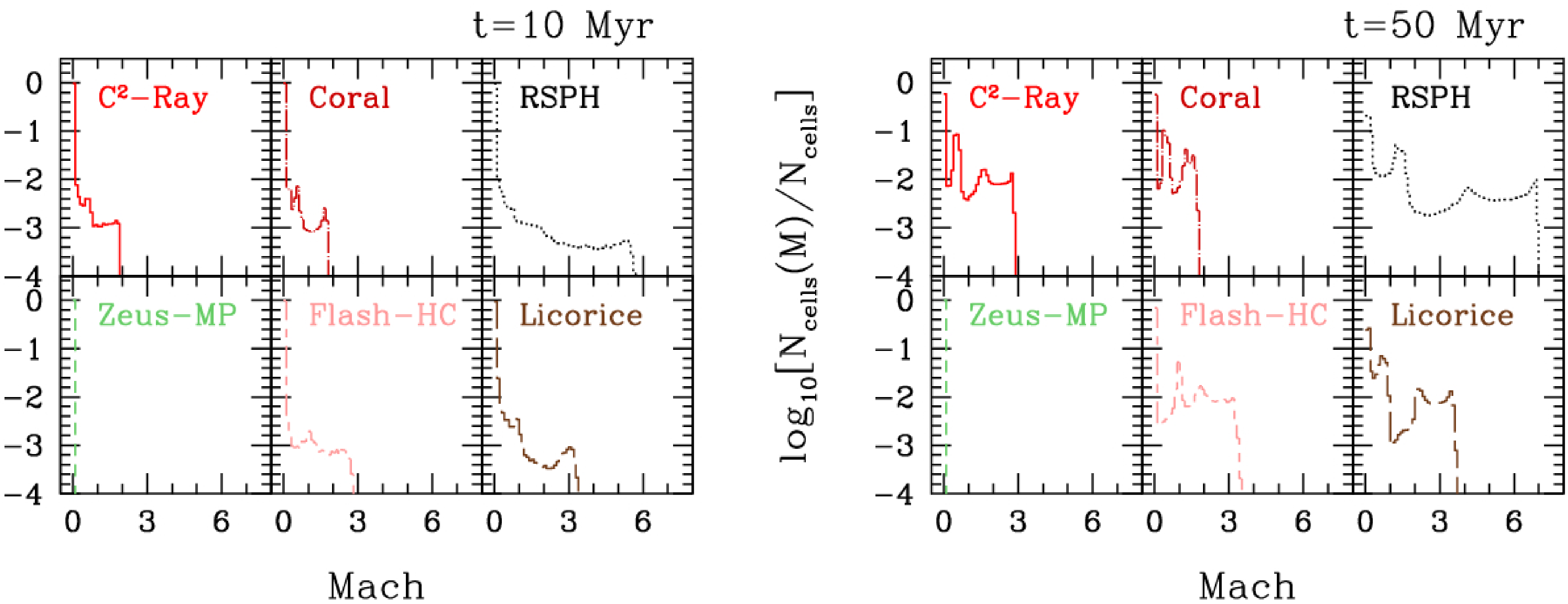

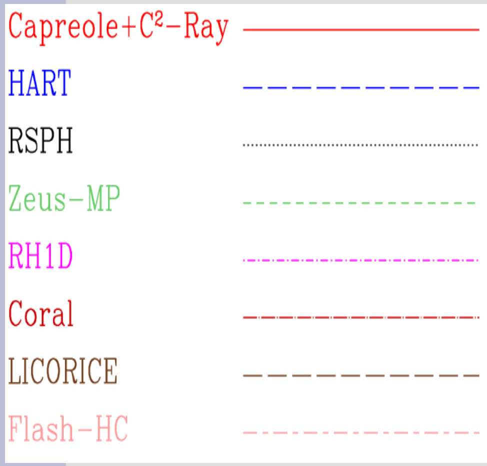

Summary

- Chemical reaction and cooling rates are still somewhat uncertain – can give up to 10-30% difference in outcome. Equilibrium chemistry is generally not a good approximation.
- All methods track I-fronts fairly well, yield reliable results. Some methods could introduce unphysical anisotropies, however.
- The largest discrepancies are due to imprecise treatments of the energy equation (temperature) and of the multi-frequency photons (spectral hardening) – the best approach is very problem-dependent.
- Radiative-hydrodynamics direct coupling – inherently more complex. Still results are relatively consistent between different methods, but there are also some significant and nontrivial variations, which require further careful study.
- It is important to evaluate the limitations of each code, some methods could underperform or even fail in certain situations